Distribution Agreement

In presenting this thesis or dissertation as a partial fulfillment of the requirements for an advanced degree from Emory University, I hereby grant to Emory University and its agents the non-exclusive license to archive, make accessible, and display my thesis or dissertation in whole or in part in all forms of media, now or hereafter known, including display on the world wide web. I understand that I may select some access restrictions as part of the online submission of this thesis or dissertation. I retain all ownership rights to the copyright of the thesis or dissertation. I also retain the right to use in future works (such as articles or books) all or part of this thesis or dissertation.

Signature:

_____ _____

Runze Li 05/01/2021

Mathematical Modeling of Thyroid Hormone Metabolism in the Human Liver

By

Runze Li

Master of Science in Public Health

Environmental Health-Epidemiology

Gangarosa Department of Environmental Health

_____

Qiang, Zhang

Committee Chair

Mathematical Modeling of Thyroid Hormone Metabolism in the Human Liver

By

Runze Li

B.A.

Emory University

2019

Thesis Committee Chair: Qiang, Zhang, M.D., Ph.D.

An abstract of

A thesis submitted to the Faculty of the
Rollins School of Public Health of Emory University

in partial fulfillment of the requirements for the degree of
Master of Science in Public Health
in Gangarosa Department of Environmental Health

2021

Mathematical Modeling of Thyroid Hormone Metabolism in the Human Liver

By Runze Li

Abstract

Background: Thyroid hormones (THs) including T_3 and T_4 play an important role in human development and energy regulation. In the liver there are three major metabolic pathways of THs including deionization by deiodinases (DIO), sulfation by sulfotransferases (SULT), and glucuronidation by glucotransferase (UGT). Many of these enzymes can be induced or inhibited by thyroid disrupting chemicals (TDCs), leading to TH-associated adverse disease outcomes. However, the quantitative effects of these hepatic perturbations on TH metabolism are unknown.

Objective: (1) Collect literature information on the kinetic parameters of hepatic DIOs, SULTs and UGTs metabolizing THs in the human liver. (2) Develop a mathematical model of TH metabolism in the liver. (3) Use the mathematical model to investigate quantitatively how TDCs-induced changes of TH metabolic enzymes would alter hepatic TH levels and metabolic fluxes.

Methods: An ordinary differential equation (ODE)-based deterministic model of TH metabolism in the liver was developed in *R*. Steady-state concentrations of various species of THs, including T_4, T_3, reverse T_3 (rT_3), T_2, and their sulfated and glucuronidated forms and the associated metabolic fluxes were calculated. Sensitivity analysis and dose-response simulations were conducted to measure the changes in THs and TH fluxes in response to changes in enzyme levels.

Results: Hepatic T_4 and T_3 levels are highly resistant to enzymatic perturbations, because the influx and efflux of T_3 and T_4 between the liver and plasma play a dominant role. In contrast, the flux from T_4 to T_3 and from T_4 to rT_3 are highly sensitive to DIO1. The flux from T_4 to T_4G is sensitive to UGT and the sensitivity is UGT1A9 > UGT1A1 > UGT1A3. The flux from T_4 to T_4S is sensitive to SULT and the sensitivity is SULT1A1 > SULT1E1. The model predicts that free T_4 is about 0.04% of total T_4 and free T_3 about 0.5% of total T_3 in the liver.

Conclusion: A mathematical model of TH metabolism in the liver can be an important tool in studying TH metabolism in the liver. It can provide new information and insights into the thyroid health risk of TDCs targeting liver enzymes.

Mathematical Modeling of Thyroid Hormone Metabolism in the Human Liver

By

Runze Li

B.A.

Emory University

2019

Thesis Committee Chair: Qiang, Zhang, M.D., Ph.D.

A thesis submitted to the Faculty of the
Rollins School of Public Health of Emory University

in partial fulfillment of the requirements for the degree of
Master of Science in Public Health
in Gangarosa Department of Environmental Health

2021

Acknowledgements

First and foremost, I want to thank my parents, Mr. Li and Mrs. Zhao. They had been supporting me to pursue in higher education and throughout the program. They also provided much love in every aspect of my life. We went through laughter and cries and they would always be right beside me when I needed them. I won't have thrived this healthy and achieve such accomplishments without them.

To my advisor, Dr. Qiang Zhang for his throughout support and dedication to the thesis. He mentored me hours on mathematical modeling and on knowledge related to thyroid hormone metabolism outside the classroom each week. This thesis would be impossible without him.

To our ADAP, Ariadne Swichtenberg. She had been providing helping hands to us throughout the program and willingly to answer, solve, and provide advice on any problems that we consult her. This program would not be this lively and organized without her.

To my friends and family who had been supportive during this journey.

Table of Contents

Introduction

Physiology of thyroid hormone

The hypothalamic–pituitary–thyroid axis (HPT axis) is a subset of the neuroendocrine system that regulates production and secretion of thyroid hormones (THs) throughout the human body. HPT axis starts with the hypothalamus where the tripeptide thyrotropin-releasing hormone (TRH) is synthesized and secreted. TRH is then delivered to the pituitary gland stimulating the synthesis and production of thyroid-stimulating hormone (TSH). TSH then stimulates the thyroid gland to synthesize and produce prohormone thyroxine (T_4) and triiodothyronine (T_3) at a ratio of about 14:1 [1].These two THs enter the blood circulation and travel to other organs [2]. THs are important in many biological functions such as development and energy regulation. THs can regulate basal metabolic rate, help stimulate bone growth in children, control body temperature, and control heart rate.

T_4 is the main circulating TH and T_3 is the main active form. Most T_3 is not produced by the thyroid gland but by converting of T_4 into T_3 in the peripheral tissue which accounts for 80% of total T_3 production of the body. Thus, the bioavailability of THs depends on the available amount of both T_4 and T_3 and on the tissue's capacity to metabolize THs [3].

Thyroid hormone metabolism in the liver

In general, there are three major established metabolic pathways for T_3 and T_4 – deiodination, sulfation, and glucuronidation (Fig.1). Deiodination is the main pathway of the three in the liver because it may account for 2/3 of T_4 metabolism [4]. All three pathways are irreversible [5]. The intermediate metabolites of the three pathways can serve as the substrates of one another. In addition, there are minor pathways of deamination and decarboxylation of THs.

Deiodination

Deiodination is categorized into two types, outer ring deiodination (ORD) and inner ring deiodination (IRD), which are defined as either removal of the iodine from the phenolic or tyrosyl ring of the TH substrate (Fig. 2) [3]. Outer-ring deiodination of T_4 result in T_3 and inner-ring deiodination rT_3. T_3 and rT_3 can then be further deiodinated into T_2 (3,3'-T_2 or 3,5-T_2). These deiodination activities are catalyzed by three enzymes: type 1 (DIO1), type 2 (DIO2), and type 3 (DIO3) deiodinase [3]. The substrates of these deiodinases are not limited to T_4, T_3, and rT_3. The conjugated products such as those sulfated and glucuronidated can also be deiodinated, with various affinities.

Type 1 Deiodinase (DIO1)

DIO1 is mainly expressed in the liver, kidney, and thyroid. In the liver, DIO1 is the main TH deiodinase expressed in liver parenchymal cells, primarily the hepatocytes. Current evidence shows that DIO1 is mainly located on the plasma membrane. DIO1 catalyzes all three THs, T_4, T_3, and rT_3, through removing the iodine in the phenolic (ORD) or tyrosyl ring (IRD). DIO1 contributes almost all production of T_3 in the liver. Recent studies have also shown that DIO1 is the only deiodinase that can deiodinate sulfated THs, such as T_4-S and T_3-S [4, 6].

Type 2 Deiodinase (DIO2)

DIO2 is mainly expressed in the brain, pituitary gland, thyroid gland and skeletal muscle, but also shows low concentrations in the liver [4]. Current evidence shows that DIO2 is mainly located on the membrane of the endoplasmic reticulum [4]. Unlike DIO1, DIO2 only participates in ORD removing phenolic ring iodine, thus converting T_4 to T_3 and rT_3 to 3,3'-T_2. Thus, DIO2 mainly contributes to the production of T_3 in the local tissue such as the brain and muscles. The majority of locally produced T_3 is believed to be mediated by DIO2. Recent studies have also shown that unlike DIO1, DIO2 does not participate in deiodination of sulfated THs [4, 6].

Type 3 Deiodinase (DIO3)

Unlike DIO1 and DIO2, DIO3 is mainly expressed in the fetal stage of human development. Thus, minimum to none DIO3 is expressed in the liver. DIO3 participates in IRD removing tyrosyl ring iodine from T_4 and T_3 turning them into rT_3 and 3,3'-T_2 respectively [4, 6]. The function of DIO3 during human development appears to protect the fetus, placenta, and pregnant uterus from overexpression of TH [4].

Sulfation

Sulfation is the step where sulfate is added to the hydroxyl group on the outer phenolic ring of the targeted THs. In the liver it mainly involves sulfotransferase including SULT1A1, SULT1B1, SULT1E1, and SULT2A1 [7]. The expression level of each in the liver are as follows: SULT1A1 3200, SULT1B1 840, SULT1E1 340, SULT2A1 1600 ng/mg per cytosol protein with SULT1A1 expressed the highest and SULT1E1 expressed the lowest [8]. One of the main functions of sulfation is to either speed up or slow down the rate at which an TH is deiodinated. For instance, T_4-S is barely deiodinated into T_3-S, but T_4-S can be more rapidly deiodinated into rT_3-S compared to their non-sulfated counterparts. Sulfated THs can also be deconjugated into their parent form in peripheral tissues where the parent form TH is needed in the specific tissue. Sulfation also increases TH transfer from the fetus to the maternal circulation, especially for glucuronidated T_2, which helps the fetal to get rid of excessive TH metabolic end product T_2 [5].

Glucuronidation

Glucuronidation is the step where the glucuronic acid is added to the hydroxyl group of the targeted THs [5]. Current evidence has shown that the UGT1A family mostly participates in the glucuronidation of T_4 and T_3 [9, 10]. Among which, UGT1A1, UGT1A3, and UGT1A9 are predominantly expressed in the liver with UGT1A1 being the major player which might be due to its high expression in the liver than the other two enzymes. Glucuronidated THs are then secreted

through the bile into gut. In the intestine, glucuronidated THs can be deconjugated by β-glucuronidase in the microbiome and reabsorbed into the serum. This serves as a reservoir for T_4 in the human body [5].

Thyroid disrupting chemicals in thyroid disease

Thyroid disruptors (TDs) or thyroid disrupting chemicals (TDCs) are a subgroup of endocrine disrupting chemicals (EDCs), which are exogeneous chemicals that can interfere with the function of the thyroid system through perturbing the metabolic pathways, production, or receptor binding of THs, etc. [11]. Major TDCs disrupting the metabolic pathways of THs include polychlorinated biphenyls (PCB), 2,3,7,8-tetrachlorodibenzo-p-dioxin (TCDD), halogenated phenolic contaminants (HOCs), and bisphenol-A (BPA).

Polychlorinated Biphenyls (PCB)

PCBs are widely used before the 1970s in many industries including plastic, paper, and electrical equipment production. Though banned since 1979, PCBs persistent in the environment are still posing threats to human health especially through food intake [12]. There have been consistent findings on the relationship between PCBs and THs. Increased exposure of PCBs is associated with decreases in the levels of total and free T_3, and T_4 in the human blood [11, 13]. More recent findings have suggested that the effects of PCBs may involve the metabolic pathway of THs. Due to PCBs' resemblance in chemical structure to THs, studies had found that PCBs compete with THs for binding with DIO [14], which implies less production of T_3, rT_3, and T_2. On top of that, PCBs can also induce the production of UGT1A1 and UGT1A6 in the rat liver [15]. This would speed up T_3 and T_4 glucuronidation resulting in less T_3 and T_4 in the liver. Hydroxylated metabolites of PCB (OH-PCB) also have a strong affinity to bind and inhibit SULT1E1 [16]. Though the binding potency of OH-PCB to SULT1E1 and SULT1A1 are different, both SULTs can be inhibited thus reducing sulfation of THs.

2,3,7,8-Tetrachlorodibenzo-p-dioxin (TCDD)

TCDD is the most toxic among polychlorinated dibenzo-p-dioxins and furans (PCDD/Fs). TCDD is mostly produced in the process of burning or synthesis of organic materials especially during the production of 2,4,5-trichlorophenol (TCP) [17]. Many epidemiological studies have shown that TCDD exposures are associated with a decrease in serum total and free T_4, but no observed changes in serum total and free T_3 and TSH [11, 13]. Further mechanistic studies have shown that TCDD reduces activity of DIO1 but increases activity of DIO2 in the rat liver which decreases T_4 but increases T_3 levels in the organ [18].

Halogenated Phenolic Contaminants (HOCs)

HOCs, particularly those used as flame retardants, are found widely in plastics and electronic equipment. Studies with mammals have shown that HOCs can bind to TH transporter proteins, thyroxine-binding globulin, and TH receptors, altering TH functionality [11, 13]. A recent study has shown that all classes of HOCs tested have various activities of inhibiting DIO1 function in the human liver [19]. A reduction in DIO1 functionality would lead to a decrease in the production of the active T_3 in the liver.

Bisphenol-A (BPA)

BPA is another chemical found ubiquitously in plastic products including toys, cosmetics, and food packaging. It has been found that there is a negative relationship between urine BPA and TSH in humans [20]. Recent studies in rodents have also shown the potential of BPA to inhibit DIO1 and DIO2 function in the liver [21] which would decrease TH metabolism and inhibit TH functioning in the organ.

Role of mathematical modeling in studying TH metabolism and thyroid diseases

Mathematical modeling is an important approach in studying thyroid disease. There has been incomplete understanding of the adverse effects of TDCs on THs which cannot be addressed efficiently by web-lab experimentation alone [2, 22]. Mathematical modeling turns biological reactions and pathways into differential equations that can track the changes of biological variables in time. By modeling, we could map out how each TH and each metabolic pathway change over time with different doses of a particular or even a mixture of TCDs. With the help of wet-lab experiments, we could derive parameters for these equations and determine the relative rate of each metabolic reaction, steady-state level of each TH in the liver, and more importantly, we can predict how these biological variables related to THs can be altered in response to a particular TDC that disrupts the metabolic pathway of THs. Moreover, because TCDs' effects on THs in the liver might be nonlinear, mapping nonlinear dose-responses with mathematical modeling would be very helpful in providing new insights to the field. So far, the majority of mathematical modeling efforts were primarily focused on the HPT axis and modeling of TH metabolism in the liver has been rarely conducted [23, 24].

Objective of this study

Given the potential of mathematical modeling in TH toxicology and the gap in liver metabolic modeling, the following aims were pursued in this thesis study:

1. Review quantitative information on TH metabolism in the liver in the literature and derive parameter values for TH metabolic modeling in the liver.
2. Develop an Ordinary Differential Equation (ODE)-based mathematical model of thyroid hormone metabolism in the liver.
3. Explore how TDCs would alter thyroid hormone metabolism quantitively with the mathematical model.

Methods

ODEs of the mathematical model of TH metabolism in the liver

A deterministic model of the TH metabolism in the liver was developed as a coupled ODEs system (Fig.3). The model contains the following state variables: T_4, T_3, rT_3, T_2, glucordinated-T_4 (T_4G), glucordinated-T_3 (T_3G), glucordinated-rT_3 (rT_3G), glucordinated-T_2 (T_2G), sulfated-T_4 (T_4S), sulfated-T_3 (T_3S), sulfated-rT_3 (rT_3S), and sulfated-T_2 (T_2S). The metabolic processes include: deiodination of T_4 to T_3, T_4 to rT_3, T_3 to T_2, rT_3 to T_2, T_4G to T_3G, T_4G to rT_3G, T_3G to T_2G, rT_3G to T_2G, T_4S to T_3S, T_4S to rT_3S, T_3S to T_2S, and rT_3S to T_2S; sulfation of T_4 to T_4S, T_3 to T_3S, rT_3 to rT_3S, and T_2 to T_2S; glucuronidation of T_4 to T_4G, T_3 to T_3G, rT_3 to rT_3G, and T_2 to T_2G. The resulting 12 ODEs are as follows:

$$\frac{dTT4}{dt} = kiT4 * fT4\_plasma / VLT - VmaxD1T4T3 * fT4/(KmD1T4T3 + fT4) - VmaxD2T4T3 * fT4/(KmD2T4T3 + fT4) - VmaxD1T4rT3 * fT4/(KmD1T4rT3 + fT4) - VmaxD3T4rT3 * fT4/(KmD3T4rT3 + fT4) - VmaxSULT1A1T4 * fT4/(KmSULT1A1T4 + fT4) - VmaxSULT1A3T4 * fT4/(KmSULT1A3T4 + fT4) - VmaxSULT1B1T4 * fT4/(KmSULT1B1T4 + fT4) - VmaxSULT1C1T4 * fT4/(KmSULT1B1T4 + fT4) - VmaxSULT1E1T4 * fT4/(KmSULT1E1T4 + fT4) - VmaxSULT2A1T4 * fT4/(KmSULT2A1T4 + fT4) - VmaxUGT1A1T4 * fT4/(KmUGT1A1T4 + fT4) - VmaxUGT1A3T4 * fT4/(KmUGT1A3T4 + fT4) - VmaxUGT1A9T4 * fT4/(KmUGT1A9T4 + fT4) - koT4 * fT4 / VLT$$

$$\frac{dTT3}{dt} = kiT3 * fT3\_plasma / VLT + VmaxD1T4T3 * fT4/(KmD1T4T3 + fT4)$$
$$+ VmaxD2T4T3 * fT4/(KmD2T4T3 + fT4) - VmaxD1T3T2$$
$$* fT3/(KmD1T3T2 + fT3) - VmaxD3T3T2 * fT3/(KmD3T3T2 + fT3)$$
$$- VmaxSULT1A1T3 * fT3/(KmSULT1A1T3 + fT3) - VmaxSULT1A3T3$$
$$* fT3/(KmSULT1A3T3 + fT3) - VmaxSULT1B1T3 * fT3/(KmSULT1B1T3$$
$$+ fT3) - VmaxSULT1C1T3 * fT3/(KmSULT1B1T3 + fT3)$$
$$- VmaxSULT1E1T3 * fT3/(KmSULT1E1T3 + fT3) - VmaxSULT2A1T3$$
$$* fT3/(KmSULT2A1T3 + fT3) - VmaxUGT1A1T3 * fT3/(KmUGT1A1T3$$
$$+ fT3) - VmaxUGT1A3T3 * fT3/(KmUGT1A3T3 + fT3) - VmaxUGT1A9T3$$
$$* fT3/(KmUGT1A9T3 + fT3) - koT3 * fT3 / VLT$$

$$\frac{dTrT3}{dt} = kirT3 + VmaxD1T4rT3 * fT4/(KmD1T4rT3 + fT4) + VmaxD3T4rT3$$
$$* fT4/(KmD3T4rT3 + fT4) - VmaxD1rT3T2 * frT3/(KmD1rT3T2 + frT3)$$
$$- VmaxD2rT3T2 * frT3/(KmD2rT3T2 + frT3) - VmaxSULT1A1rT3$$
$$* frT3/(KmSULT1A1rT3 + frT3) - VmaxSULT1A3rT3$$
$$* frT3/(KmSULT1A3rT3 + frT3) - VmaxSULT1B1rT3$$
$$* frT3/(KmSULT1B1rT3 + frT3) - VmaxSULT1C1rT3$$
$$* frT3/(KmSULT1C1rT3 + fT3) - VmaxSULT1E1rT3$$
$$* frT3/(KmSULT1E1rT3 + frT3) - VmaxSULT2A1rT3$$
$$* frT3/(KmSULT2A1rT3 + frT3) - VmaxUGT1A1rT3 * frT3/(KmUGT1A1rT3$$
$$+ frT3) - VmaxUGT1A3rT3 * frT3/(KmUGT1A3rT3 + frT3)$$
$$- VmaxUGT1A9rT3 * frT3/(KmUGT1A9rT3 + frT3) - korT3 * frT3 / VLT$$

$$\frac{dTT2}{dt} = kiT2 + VmaxD1T3T2 * fT3/(KmD1T3T2 + fT3) + VmaxD3T3T2 * fT3/(KmD3T3T2 + fT3) + VmaxD1rT3T2 * frT3/(KmD1rT3T2 + frT3) + VmaxD2rT3T2 * frT3/(KmD2rT3T2 + frT3) - VmaxSULT1A1T2 * fT2/(KmSULT1A1T2 + fT2) - VmaxSULT1A3T2 * fT2/(KmSULT1A3T2 + fT2) - VmaxSULT1B1T2 * fT2/(KmSULT1B1T2 + fT2) - VmaxSULT1C1T2 * fT2/(KmSULT1C1T2 + fT2) - VmaxSULT1E1T2 * fT2/(KmSULT1E1T2 + fT2) - VmaxSULT2A1T2 * fT2/(KmSULT2A1T2 + fT2) - VmaxUGT1A1T2 * fT2/(KmUGT1A1T2 + fT2) - VmaxUGT1A3T2 * fT2/(KmUGT1A3T2 + fT2) - VmaxUGT1A9T2 * fT2/(KmUGT1A9T2 + fT2) - koT2 * fT2 / VLT$$

$$\frac{dTT4S}{dt} = kiT4S - VmaxD1T4ST3S * fT4S/(KmD1T4ST3S + fT4S) - VmaxD2T4ST3S * fT4S/(KmD2T4ST3S + fT4S) - VmaxD1T4SrT3S * fT4S/(KmD1T4SrT3S + fT4S) - VmaxD3T4SrT3S * fT4S/(KmD3T4SrT3S + fT4S) + VmaxSULT1A1T4 * fT4/(KmSULT1A1T4 + fT4) + VmaxSULT1A3T4 * fT4/(KmSULT1A3T4 + fT4) + VmaxSULT1B1T4 * fT4/(KmSULT1B1T4 + fT4) + VmaxSULT1C1T4 * fT4/(KmSULT1C1T4 + fT4) + VmaxSULT1E1T4 * fT4/(KmSULT1E1T4 + fT4) + VmaxSULT2A1T4 * fT4/(KmSULT2A1T4 + fT4) - koT4S * fT4S / VLT$$

$$\frac{dTT3S}{dt} = kiT3S + VmaxD1T4ST3S * fT4S/(KmD1T4ST3S + fT4S) + VmaxD2T4ST3S * fT4S/(KmD2T4ST3S + fT4S) - VmaxD1T3ST2S * fT3S/(KmD1T3ST2S + fT3S) - VmaxD3T3ST2S * fT3S/(KmD3T3ST2S + fT3S) + VmaxSULT1A1T3 * fT3/(KmSULT1A1T3 + fT3) + VmaxSULT1A3T3 * fT3/(KmSULT1A3T3 + fT3) + VmaxSULT1B1T3 * fT3/(KmSULT1B1T3 + fT3) + VmaxSULT1C1T3 * fT3/(KmSULT1C1T3 + fT3) + VmaxSULT1E1T3 * fT3/(KmSULT1E1T3 + fT3) + VmaxSULT2A1T3 * fT3/(KmSULT2A1T3 + fT3) - koT3S * fT3S / VLT$$

$$\frac{dTrT3S}{dt} = kirT3S + VmaxD1T4SrT3S * fT4S/(KmD1T4SrT3S + fT4S) + VmaxD3T4SrT3S * fT4S/(KmD3T4SrT3S + fT4S) - VmaxD1rT3ST2S * frT3S/(KmD1rT3ST2S + frT3S) - VmaxD2rT3ST2S * frT3S/(KmD2rT3ST2S + frT3S) + VmaxSULT1A1rT3 * frT3/(KmSULT1A1rT3 + frT3) + VmaxSULT1A3rT3 * frT3/(KmSULT1A3rT3 + frT3) + VmaxSULT1B1rT3 * frT3/(KmSULT1B1rT3 + frT3) + VmaxSULT1C1rT3 * frT3/(KmSULT1C1rT3 + fT3) + VmaxSULT1E1rT3 * frT3/(KmSULT1E1rT3 + frT3) + VmaxSULT2A1rT3 * frT3/(KmSULT2A1rT3 + frT3) - korT3S * frT3S / VLT$$

$$\frac{dTT2S}{dt} = kiT2S + VmaxD1T3ST2S * fT3S/(KmD1T3ST2S + fT3S) + VmaxD3T3ST2S * fT3S/(KmD3T3ST2S + fT3S) + VmaxD1rT3ST2S * frT3S/(KmD1rT3ST2S + frT3S) + VmaxD2rT3ST2S * frT3S/(KmD2rT3ST2S + frT3S) + VmaxSULT1A1T2 * fT2/(KmSULT1A1T2 + fT2) + VmaxSULT1A3T2 * fT2/(KmSULT1A3T2 + fT2) + VmaxSULT1B1T2 * fT2/(KmSULT1B1T2 + fT2) + VmaxSULT1C1T2 * fT2/(KmSULT1C1T2 + fT2) + VmaxSULT1E1T2 * fT2/(KmSULT1E1T2 + fT2) + VmaxSULT2A1T2 * fT2/(KmSULT2A1T2 + fT2) - koT2S * fT2S / VLT$$

$$\frac{dTT4G}{dt} = kiT4G - VmaxD1T4GT3G * fT4G/(KmD1T4GT3G + fT4G) - VmaxD2T4GT3G * fT4G/(KmD2T4GT3G + fT4G) - VmaxD1T4GrT3G * fT4G/(KmD1T4GrT3G + fT4G) - VmaxD3T4GrT3G * fT4G/(KmD3T4GrT3G + fT4G) + VmaxUGT1A1T4 * fT4/(KmUGT1A1T4 + fT4) + VmaxUGT1A3T4 * fT4/(KmUGT1A3T4 + fT4) + VmaxUGT1A9T4 * fT4/(KmUGT1A9T4 + fT4) - koT4G * fT4G / VLT$$

$$\frac{dTT3G}{dt} = kiT3G + VmaxD1T4GT3G * fT4G/(KmD1T4GT3G + fT4G) + VmaxD2T4GT3G * fT4G/(KmD2T4GT3G + fT4G) - VmaxD1T3GT2G * fT3G/(KmD1T3GT2G + fT3G) - VmaxD3T3GT2G * fT3G/(KmD3T3GT2G + fT3G) + VmaxUGT1A1T3 * fT3/(KmUGT1A1T3 + fT3) + VmaxUGT1A3T3 * fT3/(KmUGT1A3T3 + fT3) + VmaxUGT1A9T3 * fT3/(KmUGT1A9T3 + fT3) - koT3G * fT3G / VLT$$

$$\frac{dTrT3G}{dt} = kirT3G + VmaxD1T4GrT3G * fT4G/(KmD1T4GrT3G + fT4G) + VmaxD3T4GrT3G * fT4G/(KmD3T4GrT3G + fT4G) - VmaxD1rT3GT2G * frT3G/(KmD1rT3GT2G + frT3G) - VmaxD2rT3GT2G * frT3G/(KmD2rT3GT2G + frT3G) + VmaxUGT1A1rT3 * frT3/(KmUGT1A1rT3 + frT3) + VmaxUGT1A3rT3 * frT3/(KmUGT1A3rT3 + frT3) + VmaxUGT1A9rT3 * frT3/(KmUGT1A9rT3 + frT3) - korT3G * frT3G / VLT$$

$$\frac{dTT2G}{dt} = kiT2G + VmaxD1T3GT2G * fT3G/(KmD1T3GT2G + fT3G) + VmaxD3T3GT2G * fT3G/(KmD3T3GT2G + fT3G) + VmaxD1rT3GT2G * frT3G/(KmD1rT3GT2G + frT3G) + VmaxD2rT3GT2G * frT3G/(KmD2rT3GT2G + frT3G) + VmaxUGT1A1T2 * fT2/(KmUGT1A1T2 + fT2) + VmaxUGT1A3T2 * fT2/(KmUGT1A3T2 + fT2) + VmaxUGT1A9T2 * fT2/(KmUGT1A9T2 + fT2) - koT2G * fT2G / VLT$$

Derivation of parameter values for hepatic TH metabolism

Hepatic TH Influx and Efflux

Rates of influx and efflux of T_4 and T_3 between liver blood and liver tissue and the corresponding first-order rate constants were obtained from the preliminary model developed by Dr. Zhang (unpublished). The efflux rate constants of T_4 and T_3 were re-adjusted according to the free fractions of T_4 and T_3 respectively.

Deiodination

The V_{max} and K_m values for deiodination were derived from Visser 1988 et al. [25]. In the study,

human liver tissues from four healthy individuals including one male (aged 46 years) and three females (aged 9-46 years) were used. Derivation is detailed below.

Initial K_m values

The measured K_m values for T_4-to-T_3 conversion were 1.9, 2.6, 4.8, and 4.1 μM (mean = 3350 nM); for T_4-to-rT_3 conversion 3.4 and 2.5 μM (mean = 2950 nM); for rT_3-to-T_2 conversion 0.21, 0.16, 0.33, and 0.27 μM (mean = 8.1 nM); and for T_3-to-T_2 conversion 2.8 and 2.7 μM (mean = 2750 nM).

Initial V_{max} values

For V_{max}, the values were reported as pmol/min/mg microsome protein: for T_4-to-T_3 conversion were 6.9, 5.6, 12.3, 6.8; for T_4-to-rT_3 conversion were 6.5 and 4.2; for rT_3-to-T_2 conversion were 242, 213, 225, 128; for T_3-to-T_2 conversion were 11.2 and 6.7. Because we need to obtain the V_{max} of deiodination in the liver as nmol/min/L, conversion was conducted by using an equation in Yamanaka 2007 et al. [9]:

$$Vmax_{liver} = Vmax_{microsomal} * \frac{Microsomal\ Protein}{Tissue}\left(\frac{mg}{g}\right) * \frac{Tissue}{Body\ Weight}\left(\frac{g}{kg}\right) * \frac{Body\ Weight}{Liver\ Volume}\left(\frac{kg}{L}\right). \quad (1)$$

In Eq (1), microsomal protein/liver tissue = 45 mg/g, liver tissue/Body Weight = 20 g/kg [9], and Body Weight/Liver Volume = 1/0.0257 kg/L [26] were used. After this adjustment, the V_{max} values for T_4-to-T_3 conversion were 241.63, 296.11, 430.74, and 238.13 (mean = 276.65); for T_4-to-rT_3 conversion were 227.63 and 147.08 (mean = 187.35); for rT_3-to-T_2 conversion were 8474.71, 7459.14, 7879.38, and 4482.49 (mean = 7073.93); for T_3-to-T_2 conversion were 393.22 and 234.63 (mean = 313.42) nmol/min/L liver.

Glucuronidation

UGT enzymatic kinetics has not been studied sufficiently. Kinetic parameters for T_4

glucuronidation in human liver were documented in Yamanaka 2007 et al. [9] as detailed below.

Initial K_m values

Human recombinant UGT were expressed in bacteria and their individual kinetic parameters were calculated. The K_m values for UGT1A1, UGT1A3, and UGT1A9 were 104.8, 33.2, and 24.1 μM, respectively. The overall K_m of glucuronosyltransferase activity in human liver microsomes from 12 individuals was determined to be 85.9 μM.

Initial V_{max} values

The total V_{max} of UGT activity in human liver microsomes from 12 individuals was determined to be 133.4 pmol/min/mg. Yamanaka 2007 et al. [9] have also determined a relative V_{max} ratio between major UGT isoforms using human recombinant UGT expressed in bacteria: UGT1A1:UGT1A3:UGT1A9 = 1:0.2:0.68. To derive the V_{max} ratio in the human liver in vivo, we then scaled the V_{max} ratio for recombinant UGTs by the expression level of each isoform in the human liver as determined by Margaillan 2015 et al. [27]: UGT1A1: 34.64, UGT1A3: 21.12, UGT1A9: 26.97 pmol/mg liver. The final derived human hepatic V_{max} ratio is UGT1A1:UGT1A3:UGT1A9 = 0.6055:0.0738:0.3207. Using the above total human liver microsome V_{max} 133.4 pmol/min/mg, and the final V_{max} ratio, the individual V_{max} for each of the three UGT enzymes in the human liver microsome was determined: UGT1A1 0.0808, UGT1A3 0.0098, UGT 0.0428 nmol/min/mg liver microsome.

Because we need to obtain the V_{max} of glucuronidation in the liver as nmol/min/L for the modeling, unit conversion was conducted by Eq (1) as for deiodination. After this adjustment, the V_{max} values for UGT1A1, UGT1A3, and UGT1A9 are 2828.80, 344.83, and 1497.87 nmol/min/L liver respectively, and V_{max} for total UGT is 4671.60 nmol/min/L.

Sulfation

Initial K_m and V_{max} for SULT1A1

Initial K_m and V_{max} values for SULT1A1 on the four THs were derived from Li 2001 et al. [28] and Kester 1999 et al. [29]. In Li 2001 et al. [28], recombinant human SULT1A1 enzyme expressed in COS-1 cells was used, whereas in Kester 1999 et al. [29], recombinant human SULT1A1 expressed in salmonella typhimurium was used. The K_m values for T_4 were 126 and 208 µM (mean = 167000 nM); for T_3 were 84.4, 101.3 and 29.1 µM (mean = 71600 nM); for rT_3 were 36.1 and 49.8 µM (mean = 42950 nM); for T_2 were 0.63, 0.51, 0.65 µM (mean = 580 nM). For V_{max}, only T_3 and T_2 were documented in Kester 1999 et al [29]. which were 239 and 177 pmol/min/mg protein.

Initial K_m and V_{max} for SULT1B1

Initial K_m and V_{max} values for SULT1B1 on the four THs were derived from Kester 2003 et al. [30] and Fujita 1997 et al. [31]. In Kester 2003 et al. [30], recombinant rat SULT1B1 enzyme expressed in salmonella typhimurium was used, whereas in Fujita 1997 et al., recombinant rat SULT1B1 enzyme expressed in *E. coli* was used. The average K_m values for T_3, rT_3, and T_2 from the two studies were 142, 40.2, and 7.74 µM respectively. For V_{max}, only T_3 and T_2 were documented in Kester 2003 et al. which were 1156 and 6029 pmol/min/mg protein. K_m and V_{max} values for SULT1B1 on T_4 were not determined in either of the two studies. No findings for human SULT1B1 were reported.

Initial K_m and V_{max} for SULT1E1

Initial K_m and V_{max} values for SULT1E1 on the four THs were derived from Li 1999 et al. [32], in which, recombinant human SULT1E1 enzyme expressed in COS-1 cells was used. The K_m values for T_4, T_3, rT_3, and T_2 were 13.6, 60.7, 4.63, and 9.73 µM, respectively. For V_{max} for T_4, T_3, rT_3, and T_2 were 0.4, 1.78, 15.3, and 28.5 nmol/h/mg protein respectively.

Initial K_m and V_{max} for SULT2A1

Initial K_m and V_{max} values for SULT2A1 on the four THs were derived from Li 1999 et al. [32], in which recombinant human SULT2A1 enzyme expressed in COS-1 cells was used. The K_m values for T_3, rT_3, and T_2 were 14.3, 7.05, and 25.675 μM respectively. The V_{max} values for T_3, rT_3, and T_2 were 0.13, 0.04, and 0.255 nmol/h/mg protein respectively. Neither K_m and V_{max} values were detected for T_4 in this study.

Further adjustments according to expression ratio

Because all these experiments above were using recombinant strains and expressed in non-human cells, the initial parameters values so obtained for SULTs cannot be used directly in our model. Thus, these values were first adjusted according to the enzyme expression ratio in the human liver. The expression values were determined by Riches 2009 et al. [8] using cytosol from 28 human livers: 3200 SULT1A1, 840 SULT1B1, 340 SULT1E1, and 1600 SULT2A1 ng/mg cytosol protein. Because among all four enzymes, only SULT1E1 has all the K_m and V_{max} values for the four THs without any missing parameter value, we used it as the standard or unit 1. This gives us the expression ratio of SULTs in the liver as follows: SULT1A1:SULT1B1:SULT1E1:SULT2A1 = 9.41:2.47:1:7.65. Using this ratio to adjust our previous V_{max} gave us SULT1A1 on T_4: 1.31; SULT1E1 on T_4: 0.00067; SULT1A1 on T_3: 2.25; SULT1B1 on T_3: 2.856; SULT1E1 on T_3: 0.0297; SULT2A1 on T_3: 0.0166; SULT1A1 on rT_3:1.855; SULT1B1 on rT_3:3.14; SULT1E1 on rT_3: 0.255; SULT2A1 on rT_3: 0.005098; SULT1A1 on T_2: 1.666; SULT1B1 on T_2: 14.895; SULT1E1 on T_2: 0.475; and SULT2A1 on T_2: 0.0325 nmol/min/mg protein.

Determination of free fraction of THs in the liver and enzymatic parameter fine tuning

Free fraction is the percentage of THs in the liver that participates in the reactions with DIOs, UGTs, and SULTs. Since the study by Yamanaka 2017 et al. [9] used liver tissues from 12 human individuals, the largest among all the studied cited so far, we assumed that the parameters determined by this study is more reliable than others. We therefore started determining the free fraction of T_4 by using this study as detailed below.

According to Peeters 2017 et al. [4], we made the following assumption that the hepatic T_4 metabolism by SULT and UGT accounts for 1/3 of total T_4 hepatic metabolism, which is equally split between SULT and UGT. Therefore, UGT accounts for 1/6 of total T_4 hepatic metabolism. Based on Zhang's unpublished model, in a human individual with a body weight of 75 kg, the total T_4 hepatic metabolic flux is about 5.6E-4 nmol/sec, 1/6 of which is = 9.33E-5 nmol/sec.

Using the V_{max} of total UGT 4671.60 nmol/min/L derived above, in a human individual with a body weight of 75 kg, the V_{max} is about 150.08 nmol/sec/75 kg BW. With K_m=85.9E3 nM and the liver Total T_4 concentration of 226 nM, if free T_4 is 100% of total T_4 in the liver, then the hepatic glucuronidation rate will be 0.39 nmol/sec/75kg BW. Since the expected glucuronidation rate is only 9.33E-5 nmol/sec, we argued that free T_4 must be a small fraction of total T_4 in the liver. As a result, the free fraction of T_4 was estimated to be 2.4E-4.

According to Peeters 2017 et al. [4] the fluxes from T_4 to T_3 and T_4 to rT_3 were both 1/3 of the total flux of T_4. When applying this free fraction value for T_4, the flux of deiodination is about 50% of the targeted 2/3 of the total flux of T_4 metabolism. We decided to increase the free fraction of T_4 to 4E-4, and adjusted the V_{max} values for all reactions to finally arrive at a fraction of 1/3 for T_4 to T_3, 1/3 for T_4 to rT_3, 1/6 for T_4 to T_4G, and 1/6 for T_4 to T_4S. The final parameter values are presented in Table 1. The free fraction of T_3 was determined in a similar fashion.

Sensitivity Analysis

To determine the sensitivity of each TH and each metabolic flux to changes in the level of enzymes including DIO, SULT, and UGT, we varied each enzyme's V_{max} value by increasing and decreasing 5% from the default. The average ratio of the percentage change in steady-state levels of THs and fluxes to the percentage change (5%) in V_{max} of each enzyme was calculated as the sensitivity coefficient.

Simulation Software

The programming language R was used for the deterministic simulation by using the package "deSolve" and "lsoda" ODE solver function.

Results

Steady-state Levels of THs and Fluxes

Under the basal condition, the concentrations of the THs are as follows (Fig. 4): TT_4 226.45, fT_4 0.091, TT_3 3.52, fT_3 0.018, TrT_3 1.9E-5, TT_2 3.45, TT_4S 5.2E-5, TT_3S 6.16E-4, TrT_3S 1.06E-5, TT_2S 12.46, and TT_4G 3.02 nM.

Under the basal condition, T_3 and T_4 fluxes are as follows (Fig. 5). T_4 influx 6.84, T_4 efflux 6.81, T_4 to T_3 0.011, T_4 to rT_3 0.011, T_4 to T_4S 0.0055, T_4 to T_4G 0.0055, T_3 influx 0.75, T_3 efflux 0.75, T_3 to T_2 0.0034, and T_3 to T_3S 0.0084 nmol/min.

Sensitivity Analysis

The result of sensitivity analysis on steady-state THs are presented in Fig. 6. fT_3 and TT_3 are mostly sensitive to changes in DIO1, SULT1A1, SULT1B1, SULT2A1, and SULT1E1; both fT_4 and TT_4 are mostly sensitive to changes in DIO1, SULT1A1, UGT1A9, UGT1A1, and UGT1A3; rT_3 is mostly sensitive to changes in DIO1, SULT1A1, UGT1A9, UGT1A1, and UGT1A3.

The result of sensitivity analysis on steady-state T_4 flux are presented in Fig. 7. T_4 efflux is most sensitive to changes in DIO1 SULT1A1, UGT1A9, UGT1A1, and UGT1A3; T_4 to T_3 flux and T_4 to T_4S flux are mostly sensitive to changes in DIO1; T_4 to rT_3 flux is mostly sensitive to changes in DIO1; T_4 to T_4S flux is mostly sensitive to changes in SULT1A1, SULT1E1, and DIO1; T_4 to T_4G flux is mostly sensitive to UGT1A9, UGT1A1, UGT1A3, DIO1, and SULT1A1.

Dose-response Analysis

As the DIO1 level increases, TT_3 increases and TT_4 decreases slightly (Fig. 8). Changes in the DIO1 levels have a dramatic effect on T_4 to T_3 and T_4 to rT_3 fluxes with little impact on T_4 efflux, T_4 to T_4S, and T_4 and T_4G fluxes (Fig. 9).

As the SULT1A1 level increases, TT_3 decreases slightly and there is no effect on TT_4 (Fig. 10). Changes in the SULT1A1 levels have a dramatic effect on T_4 to T_4S flux with little impact on T_4 efflux, T_4 to T_3, T_4 to rT_3, and T_4 to T_4G fluxes (Fig.11).

As the SULT1E1 level increases, there is no effect on TT_3 and TT_4 (Fig. 12). Changes in the SULT1E1 levels have a dramatic effect on T_4 to T_4S flux with little impact on T_4 efflux, T_4 to T_3, T_4 to rT_3, and T_4 to T_4G fluxes (Fig. 13). The increase in the T_4 to T_4S flux reaches nearly 5-fold when SULT1E1 levels increase by 100-fold. However, the increase in this flux is much smaller than the 15-fold increase when SULT1A1 levels increase by 100-fold.

As the UGT1A1 level increases, there is no effect on TT_3 and TT_4 (Fig. 14). Changes in the UGT1A1 levels have a dramatic effect on T_4 to T_4G flux with little impact on T_4 efflux, T_4 to T_3, T_4 to rT_3, and T_4 to T_4S fluxes (Fig. 15).

As the UGT1A3 level increases, there is no effect on TT_3 and TT_4 (Fig. 16). Changes in the UGT1A3 levels have a dramatic effect on T_4 to T_4G flux with little impact on T_4 efflux, T_4 to T_3, T_4 to rT_3, and T_4 to T_4S fluxes (Fig. 17). The increase in the T_4 to T_4S flux reaches nearly 10-fold when UGT1A3 levels increase by 100-fold. However, the increase in this flux is much smaller than the 15-fold increase when UGT1A1 levels increase by 100-fold.

As the UGT1A9 level increases, there is no effect on TT_3 and TT_4 (Fig. 18). Changes in the UGT1A9 levels have a dramatic effect on T_4 to T_4G flux with little impact on T_4 efflux, T_4 to T_3, T_4 to rT_3, and T_4 to T_4S fluxes (Fig.19). The increase in the T_4 to T_4S flux reaches nearly 15-fold when UGT1A3 levels increase by 100-fold. The increase in this flux is similar to the increase when UGT1A1 levels increase by 100-fold but higher when UGT1A3 levels increase by 100-fold.

Discussion

Environmental chemicals play an important role in TH-associated diseases by altering the liver enzymes catalyzing TH metabolism. It was estimated that liver is responsible for 1/3 of the T_4 clearance. In this study, we have developed a mathematical model of TH metabolism in the liver to aim at understanding the disruption of TH metabolism by TDCs. We searched extensively through the literature of hepatic TH metabolism and synthesized them into initial parameter values that were used in the mathematical model.

With the mathematical model we demonstrated that when the plasma T_3 and T_4 are fixed at constant levels, the hepatic steady-state T_3 and T_4 levels are extremely insensitive to changes in the abundance or activity of DIOs, SULTs and UGTs (Fig. 6). This is because the influx from and efflux into the plasma of THs, especially T_4, dominate such that the clearance fluxes are less than 5% of the influx and efflux (Fig. 5). As a result, T_3 and T_4 levels in the liver are primarily determined by the influx and efflux, while the metabolic processes, including deionization, sulfation, and glucuronidation, play only a minor role. Despite the insensitivity, we found that free and total T_3 can be increased slightly by DIO1 or decreased by SULTs and UGTs, however free and total T_4 and rT_3 can only be decreased by these enzymes when their abundance or activities increase. The unidirectional change in T_4 can be explained by the fact that there are no other influxes into T_4 than the plasma influx, therefore when increasing the metabolic enzymes, T_4 would always be decreased. Patterns in free and total T_3 can be explained by the fact that the metabolic step of converting T_4 to T_3 is a relative dominant process which would always increase T_3 concentration despite that other metabolic steps are all consuming T_3. Patterns in rT_3 can be explained by the fact that the metabolic step of converting T_4 to rT_3 is not as strong as the metabolic step of converting rT_3 to T_2. Thus, more rT_3 is consumed than produced by DIO1 increases leading to a decrease in total rT_3 concentration in all scenarios. That the hepatic T_3 and T_4 levels are insensitive to changes in these enzyme levels have important implications in

understanding and predicting the toxic effect of TDCs. It suggests that TDCS may induce the liver enzymes to increase the overall TH clearance from the entire body, however, the local TH concentrations may remain relatively constant, rejecting perturbations induced through altered metabolism.

We also made an interesting finding on the free fractions of T_3 and T_4 in the liver. Literature suggests that a large majority of T_3 and T_4 in the liver are not free but no quantitative information has been provided. Here we found that free T_4 is 0.04% of total T_4 and free T_3 is 0.5% of total T_3 in the liver, which implies only a tiny amount of T_3 and T_4 are subject to deionization, sulfation, and glucuronidation. These free fractions were calculated to ensure that given the enzymatic parameters obtained from the literature as detailed in the Methods, the total T_3 and T_4 liver concentrations can be matched to targeted values. It is unclear how close the estimated free fraction values may be to the true values in the liver, which remain to be determined in future studies.

There are few studies quantifying the relative fluxes related to T_3 and T_4 metabolism in the liver. Peeters et al speculated that overall, in the body, the ratio of metabolic steps of T_4 to T_3, T_4 to rT_3, and other remaining metabolic steps including sulfation and glucuronidation is at a ratio of about 1:1:1 [4]. In our modeling process, we have assumed this to be the case but also assuming sulfation and glucuronidation evenly divide the remaining 1/3 of the total T_4 flux. To achieve this level of sulfation, i.e., 1/6 of T_4 clearance, we had to increase the corresponding V_{max} of SULTs by over 1000-fold. This suggest that sulfation may play a minimal role in T_4 metabolism in the liver, and glucuronidation is responsible for the most conjugation of T_4.

Although we strived to obtain parameter values as much as available in the literature, not all parameter values can be found, which contributes to the uncertainty of the model. First, there

were many parameter values determined from non-human studies ranging from rats to mammals. Inter-species differences in these parameters can incorrectly parameterize the model. Second and similarly, there are some parameter values derived from studies using recombinant human enzymes and expressed in either *E. coli* or other bacteria. The expression levels of the recombinant enzymes can be very different than what is in a human liver. Thus, the estimated V_{max} may be over or under-predicting the actual values in human. Third, there are many missing parameter values including those for glucuronidation of T_3, rT_3, and T_2, and the enzyme isoforms participating in these glucuronidation processes are unknown. There are also no data on sulfation rate in human liver which we had to manually adjust them accordingly. Data on T_3, rT_3, and T_2 flux allocation is also missing. Thus, we could not adjust as accurately as T_4 flux. Deiodination process and related kinetic parameter values for glucuronidation and sulfation of THs are also not reported in the literature. For now, we can only more accurately describe how T_4 is metabolized. Fourth, we had been assuming UGT and SULT to act as monomers and based our calculation of V_{max} on this assumption. However, there has been information on whether UGT and SULT are monomers, dimers, or even heterodimers and whether the biological process depends on a single monomer or dimers/heterodimers. Nonetheless, since the model was also constrained by other metrics such as TH levels and flux levels, the uncertainty in these parameters is not expected to be large.

There are several assumptions we made about the model. We fixed the plasma THs at constant levels. In reality, the plasma levels of THs are supposed to be changing as the liver metabolism is altered. However, within the range of perturbation potentially exerted by environmental TDCs, the changes in plasma TH levels are expected to be adequately compensated by the HPT feedback regulation, which suggests that our finding of insensitivity of hepatic TH levels to enzyme activity or abundance changes may still hold true.

The intracellular TH concentrations are also under homeostatic control through multiple local feedback regulations between TH and the expression of DIOs, SULTs, UGTs and potentially other related enzymes. For instance, T_3 induces DIO1 transcription by binding to two TREs in the promoter of DIO1 gene [33]. Such local feedback mechanism can potentially maintain THs levels further when their metabolism is perturbed. Future models will need to consider these local regulations to make more accurate predictions of TH level changes.

References

1. Pilo, A., et al., *Thyroidal and peripheral production of 3,5,3'-triiodothyronine in humans by multicompartmental analysis.* Am J Physiol, 1990. **258**(4 Pt 1): p. E715-26.
2. Zoeller, R.T., S.W. Tan, and R.W. Tyl, *General background on the hypothalamic-pituitary-thyroid (HPT) axis.* Crit Rev Toxicol, 2007. **37**(1-2): p. 11-53.
3. van der Spek, A.H., E. Fliers, and A. Boelen, *The classic pathways of thyroid hormone metabolism.* Mol Cell Endocrinol, 2017. **458**: p. 29-38.
4. Peeters, R.P. and T.J. Visser, *Metabolism of Thyroid Hormone*, in *Endotext*, K.R. Feingold, et al., Editors. 2000: South Dartmouth (MA).
5. Wu, S.Y., et al., *Alternate pathways of thyroid hormone metabolism.* Thyroid, 2005. **15**(8): p. 943-58.
6. Luongo, C., M. Dentice, and D. Salvatore, *Deiodinases and their intricate role in thyroid hormone homeostasis.* Nat Rev Endocrinol, 2019. **15**(8): p. 479-488.
7. Gamage, N., et al., *Human sulfotransferases and their role in chemical metabolism.* Toxicol Sci, 2006. **90**(1): p. 5-22.
8. Riches, Z., et al., *Quantitative evaluation of the expression and activity of five major sulfotransferases (SULTs) in human tissues: the SULT "pie".* Drug Metab Dispos, 2009. **37**(11): p. 2255-61.
9. Yamanaka, H., et al., *Glucuronidation of thyroxine in human liver, jejunum, and kidney microsomes.* Drug Metab Dispos, 2007. **35**(9): p. 1642-8.
10. Meech, R., et al., *The UDP-Glycosyltransferase (UGT) Superfamily: New Members, New Functions, and Novel Paradigms.* Physiol Rev, 2019. **99**(2): p. 1153-1222.
11. Calsolaro, V., et al., *Thyroid Disrupting Chemicals.* Int J Mol Sci, 2017. **18**(12).
12. EPA. [cited 2021 May 01]; Available from: https://www.epa.gov/pcbs/learn-about-polychlorinated-biphenyls-pcbs.
13. Boas, M., et al., *Environmental chemicals and thyroid function.* Eur J Endocrinol, 2006. **154**(5): p. 599-611.
14. Marsan, E.S. and C.A. Bayse, *Halogen Bonding Interactions of Polychlorinated Biphenyls and the Potential for Thyroid Disruption.* Chemistry, 2020. **26**(23): p. 5200-5207.
15. Vansell, N.R. and C.D. Klaassen, *Increase in rat liver UDP-glucuronosyltransferase mRNA by microsomal enzyme inducers that enhance thyroid hormone glucuronidation.* Drug Metab Dispos, 2002. **30**(3): p. 240-6.
16. Wang, L.Q. and M.O. James, *Inhibition of sulfotransferases by xenobiotics.* Curr Drug Metab, 2006. **7**(1): p. 83-104.
17. CDC. [cited 2021 May 01]; Available from: https://www.cdc.gov/niosh/docs/84-104/default.html.
18. Viluksela, M., et al., *Tissue-specific effects of 2,3,7,8-tetrachlorodibenzo-p-dioxin (TCDD) on the activity of 5'-deiodinases I and II in rats.* Toxicol Lett, 2004. **147**(2): p. 133-42.
19. Butt, C.M., D. Wang, and H.M. Stapleton, *Halogenated phenolic contaminants inhibit the in vitro activity of the thyroid-regulating deiodinases in human liver.* Toxicol Sci, 2011. **124**(2): p. 339-47.
20. Meeker, J.D. and K.K. Ferguson, *Urinary phthalate metabolites are associated with decreased serum testosterone in men, women, and children from NHANES 2011-2012.* J Clin Endocrinol Metab, 2014. **99**(11): p. 4346-52.
21. da Silva, M.M., et al., *Inhibition of Type 1 Iodothyronine Deiodinase by Bisphenol A.* Horm Metab Res, 2019. **51**(10): p. 671-677.
22. Crofton, K.M., *Thyroid disrupting chemicals: mechanisms and mixtures.* Int J Androl, 2008. **31**(2): p. 209-23.

23. Kohn, M.C., *Effects of TCDD on thyroid hormone homeostasis in the rat.* Drug Chem Toxicol, 2000. **23**(1): p. 259-77.
24. Berberich, J., et al., *Mathematical Modeling of the Pituitary-Thyroid Feedback Loop: Role of a TSH-T3-Shunt and Sensitivity Analysis.* Front Endocrinol (Lausanne), 2018. **9**: p. 91.
25. Visser, T.J., et al., *Deiodination of thyroid hormone by human liver.* J Clin Endocrinol Metab, 1988. **67**(1): p. 17-24.
26. Brown, R.P., et al., *Physiological parameter values for physiologically based pharmacokinetic models.* Toxicol Ind Health, 1997. **13**(4): p. 407-84.
27. Margaillan, G., et al., *Multiplexed Targeted Quantitative Proteomics Predicts Hepatic Glucuronidation Potential.* Drug Metab Dispos, 2015. **43**(9): p. 1331-5.
28. Li, X., et al., *Characterization of human liver thermostable phenol sulfotransferase (SULT1A1) allozymes with 3,3',5-triiodothyronine as the substrate.* J Endocrinol, 2001. **171**(3): p. 525-32.
29. Kester, M.H., et al., *Characterization of human iodothyronine sulfotransferases.* J Clin Endocrinol Metab, 1999. **84**(4): p. 1357-64.
30. Kester, M.H., et al., *Characterization of rat iodothyronine sulfotransferases.* Am J Physiol Endocrinol Metab, 2003. **285**(3): p. E592-8.
31. Fujita, K., et al., *Molecular cloning and characterization of rat ST1B1 and human ST1B2 cDNAs, encoding thyroid hormone sulfotransferases.* J Biochem, 1997. **122**(5): p. 1052-61.
32. Li, X. and R.J. Anderson, *Sulfation of iodothyronines by recombinant human liver steroid sulfotransferases.* Biochem Biophys Res Commun, 1999. **263**(3): p. 632-9.
33. Zavacki, A.M., et al., *Type 1 iodothyronine deiodinase is a sensitive marker of peripheral thyroid status in the mouse.* Endocrinology, 2005. **146**(3): p. 1568-75.

Tables and figures

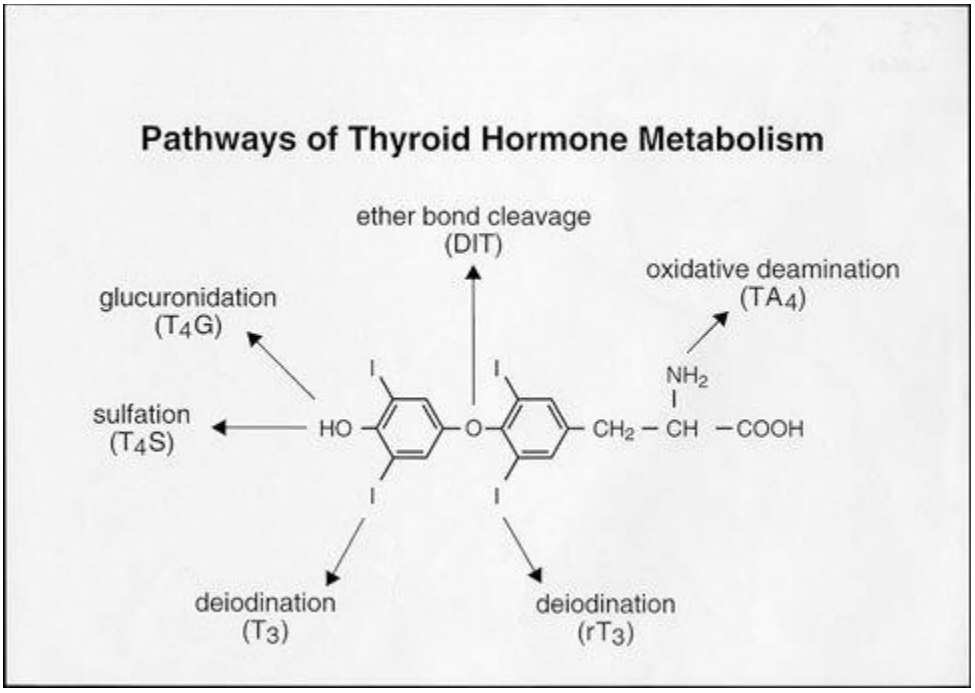

Figure 1. Major metabolic pathways of thyroid hormone metabolism (Peeters et al.)

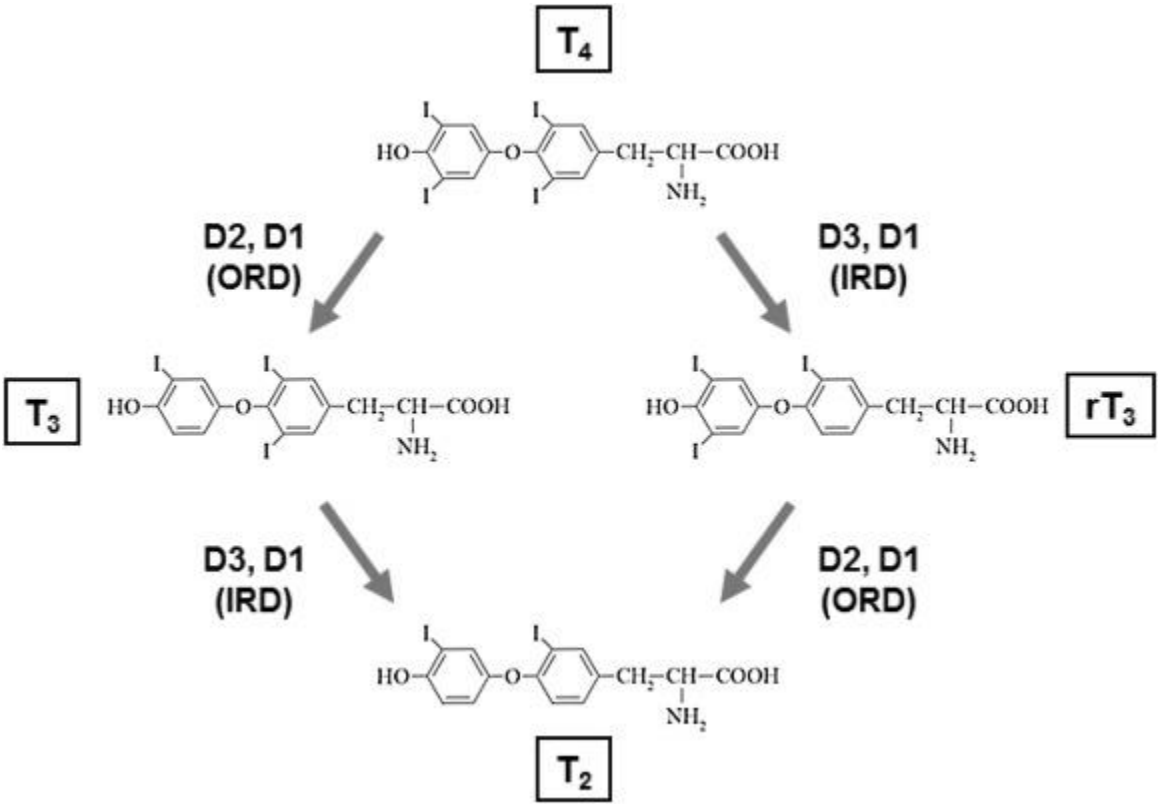

Figure 2. Deionization pathway of thyroid hormone (Van de spek et al.)

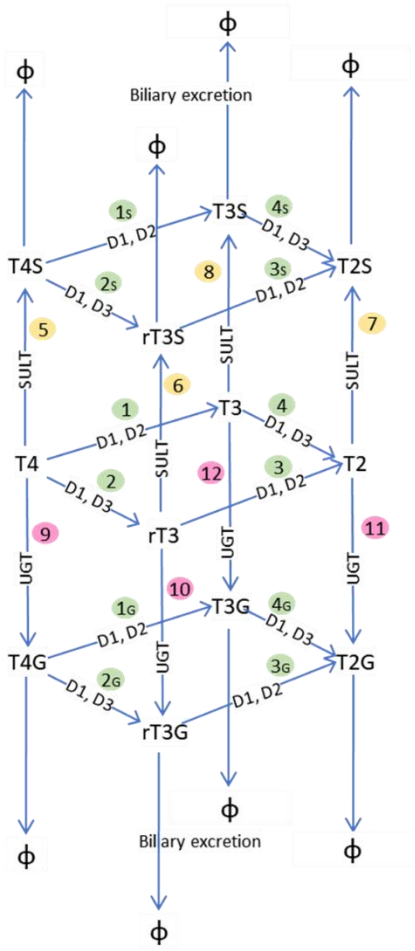

Figure 3. Schematic illustration of the mathematical model of TH metabolism in the liver.

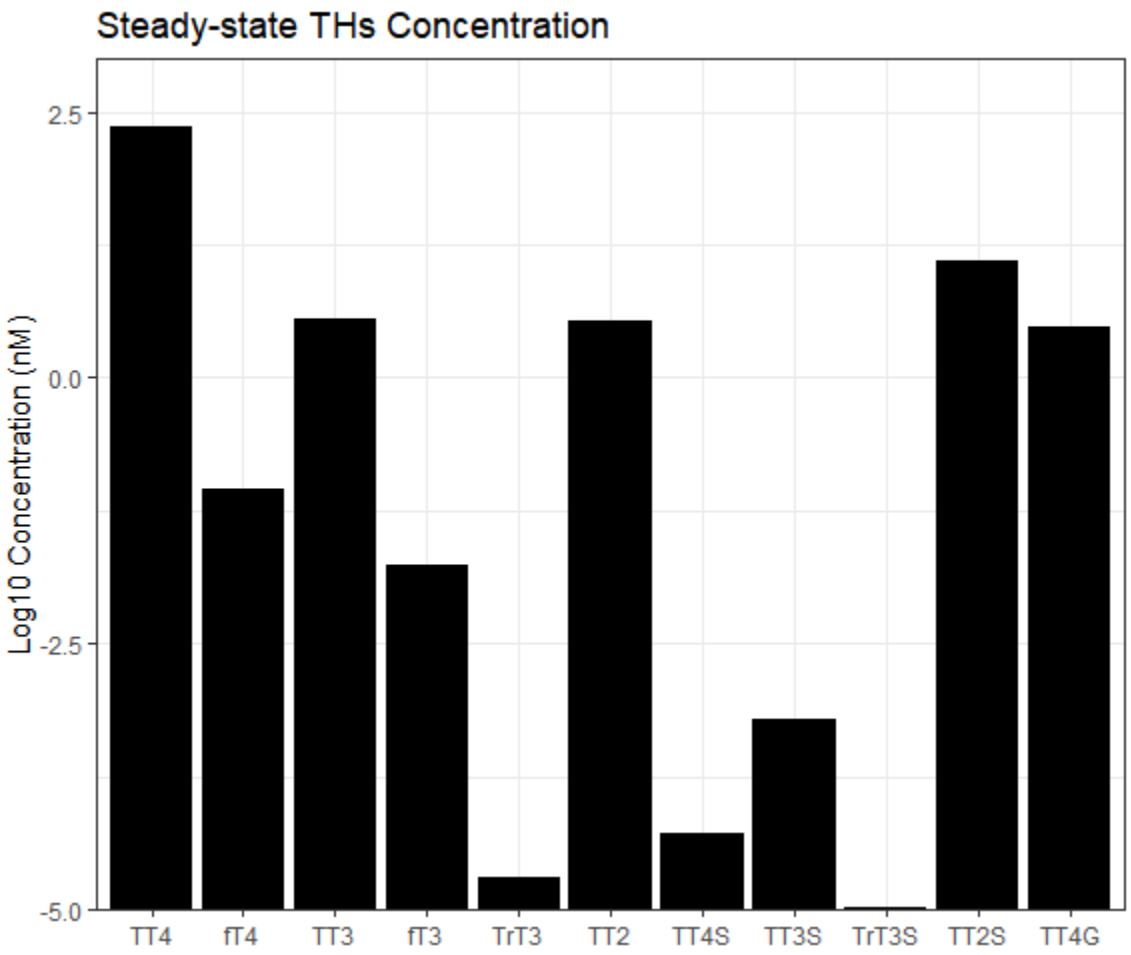

Figure 4. Steady-state TH concentrations in the liver.

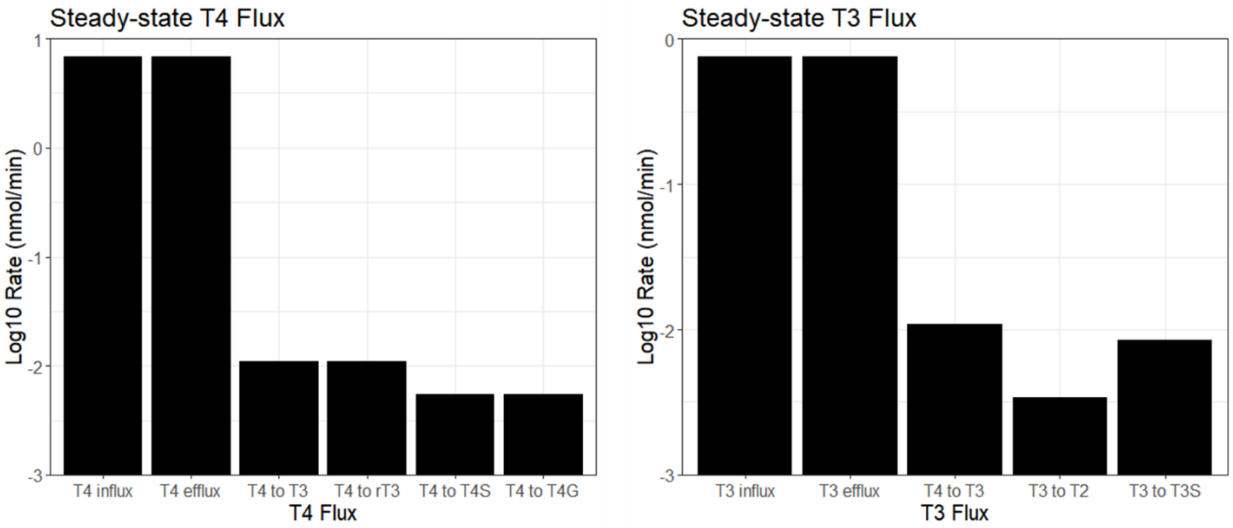

Figure 5. Steady-state fluxes of T_3 and T_4 in the liver.

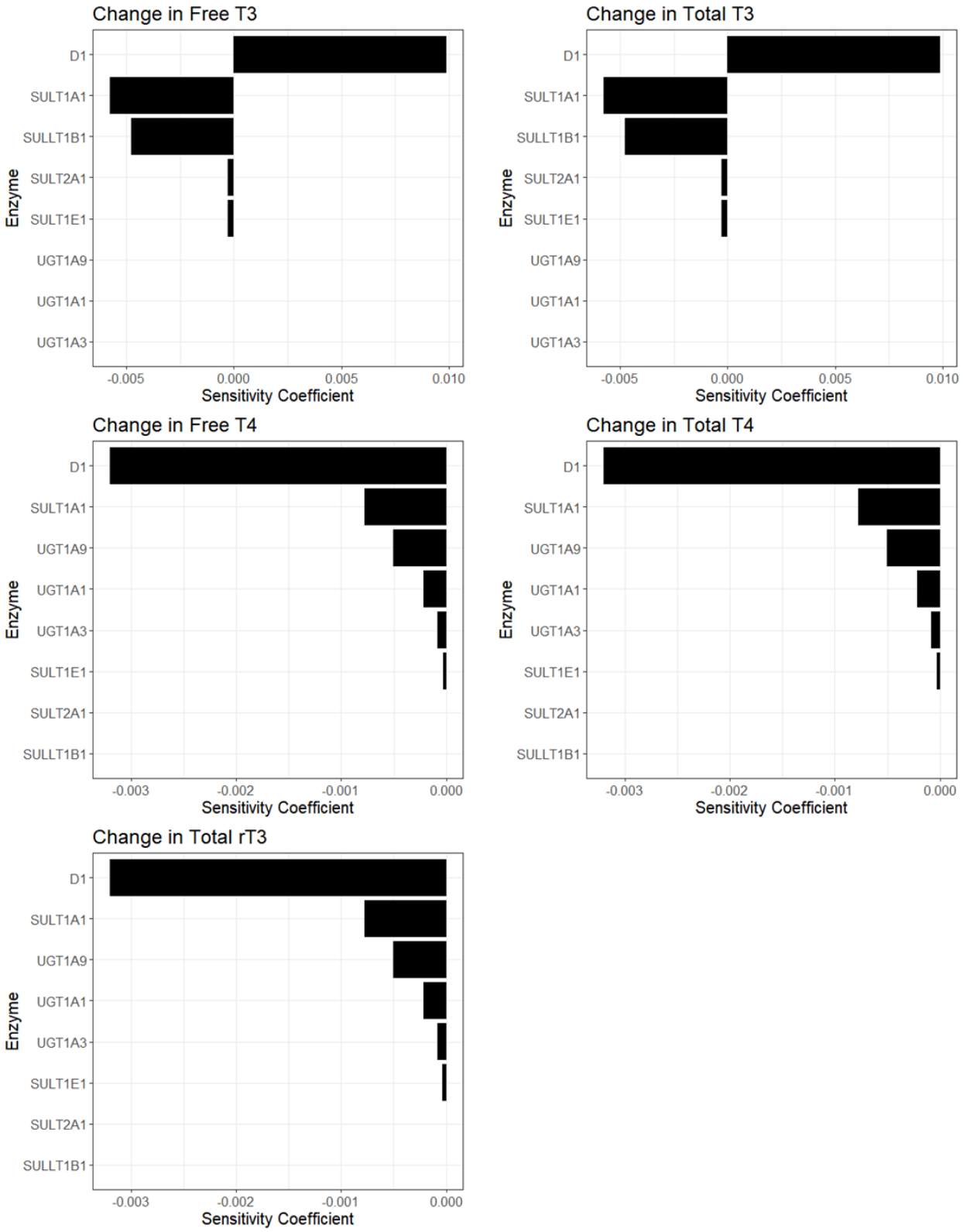

Figure 6. Sensitivity analysis for TH levels in the liver in response to changes in metabolic enzyme levels.

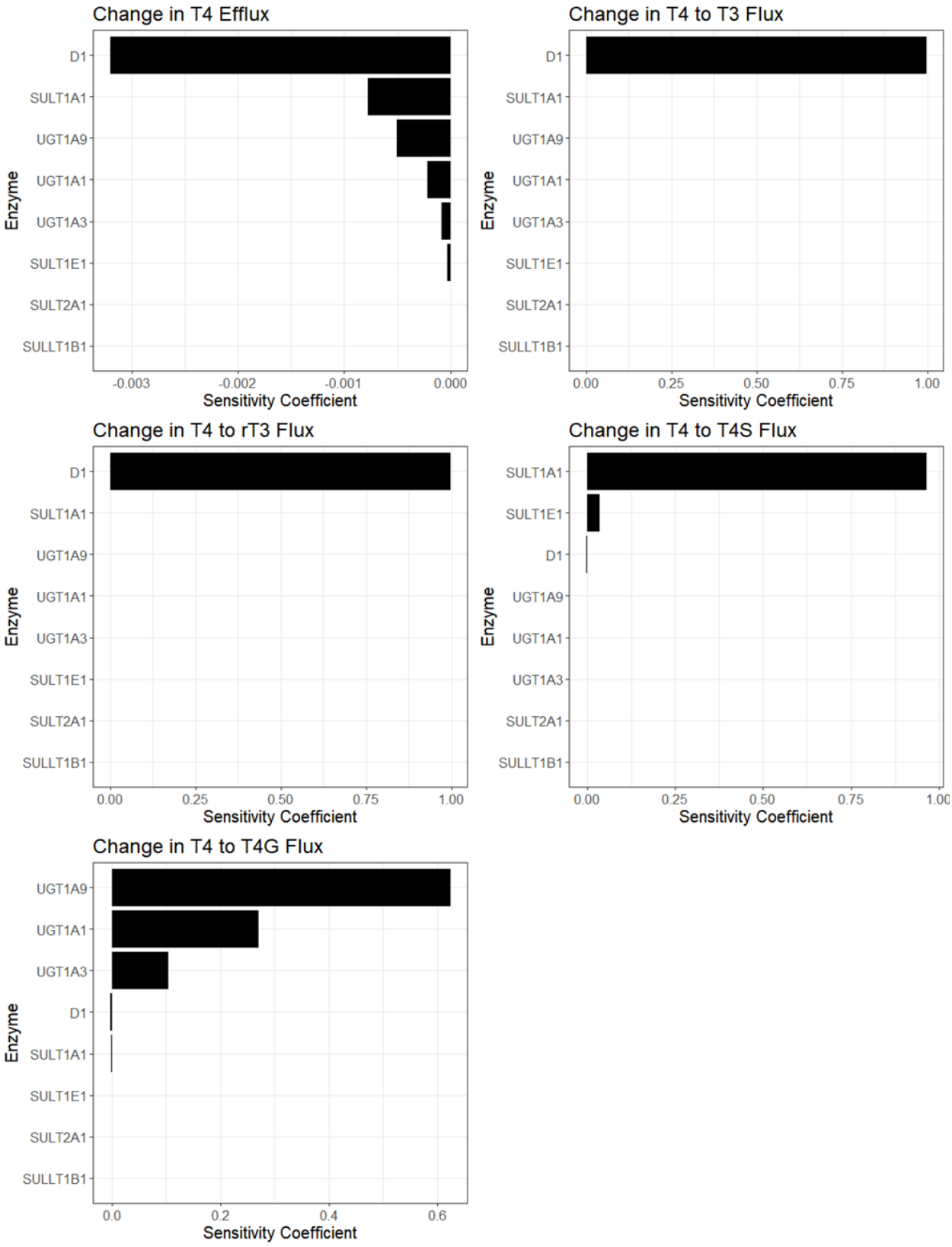

Figure 7. Sensitivity analysis for TH fluxes in the liver in response to changes in metabolic levels.

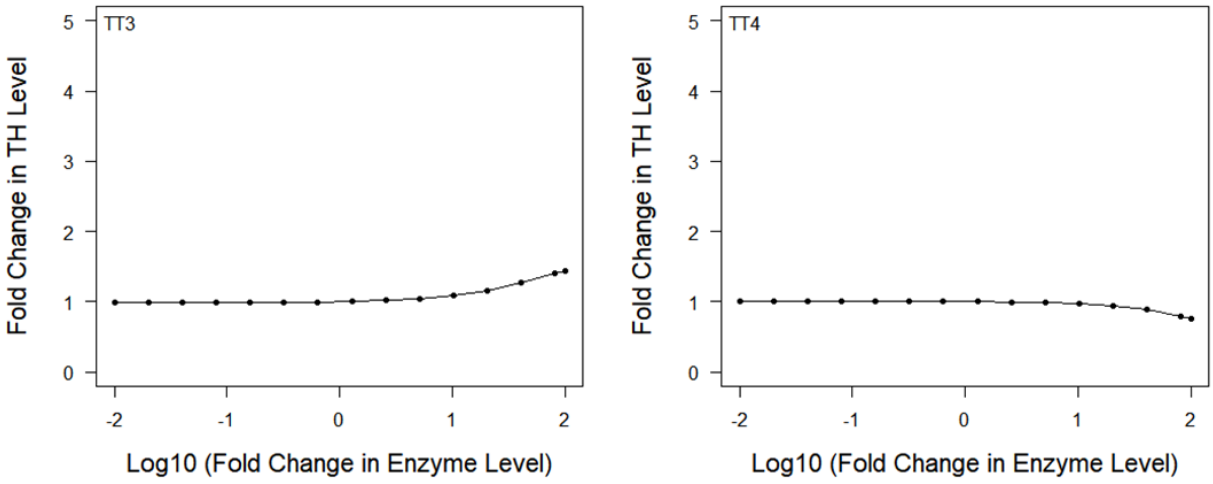

Figure 8. Steady-state dose-response of total T_3 and total T_4 to changes in DIO1 in the liver.

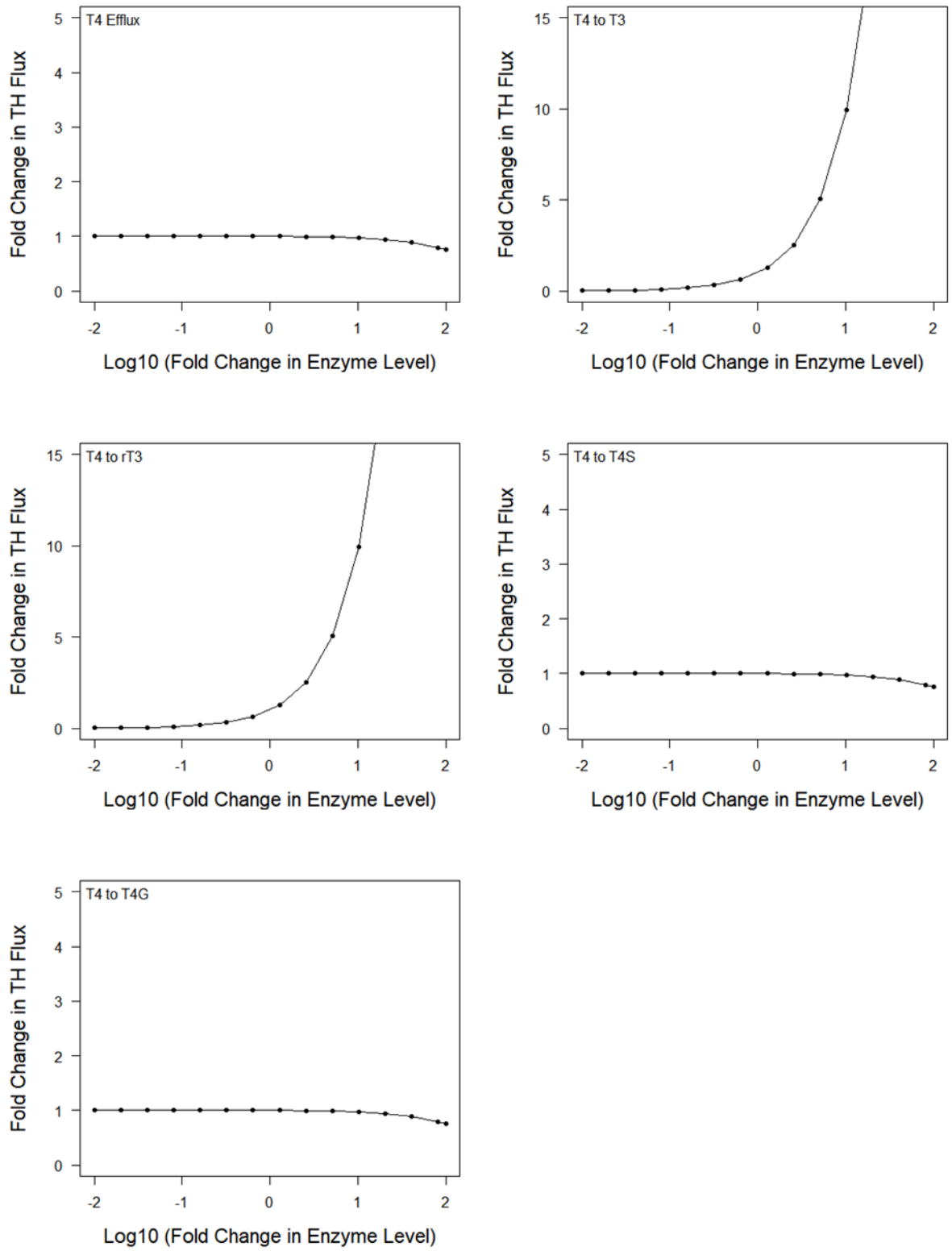

Figure 9. Steady-state dose-response of T_4-related fluxes to changes in DIO1 in the liver.

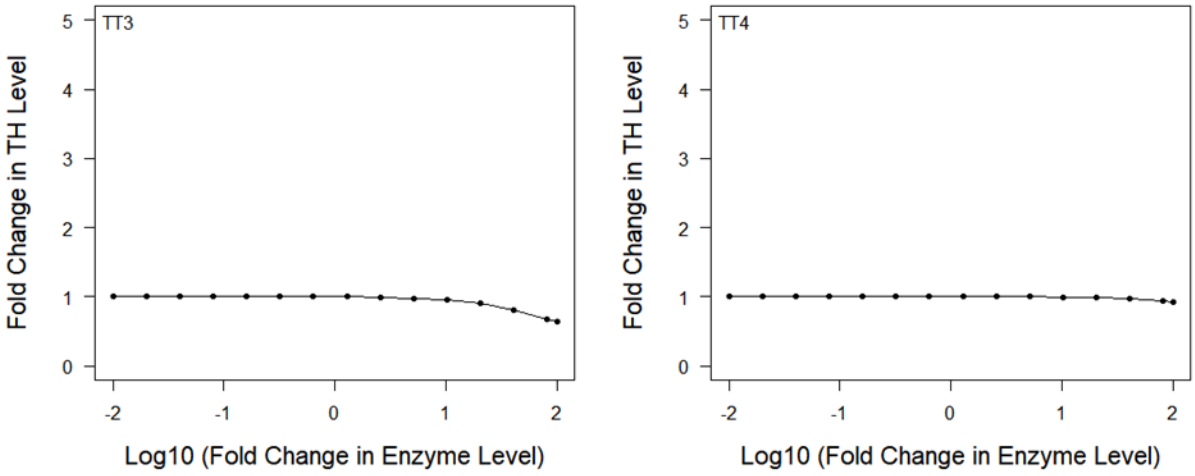

Figure 10. Steady-state dose-response of Total T_3 and T_4 to changes in SULT1A1 in the liver.

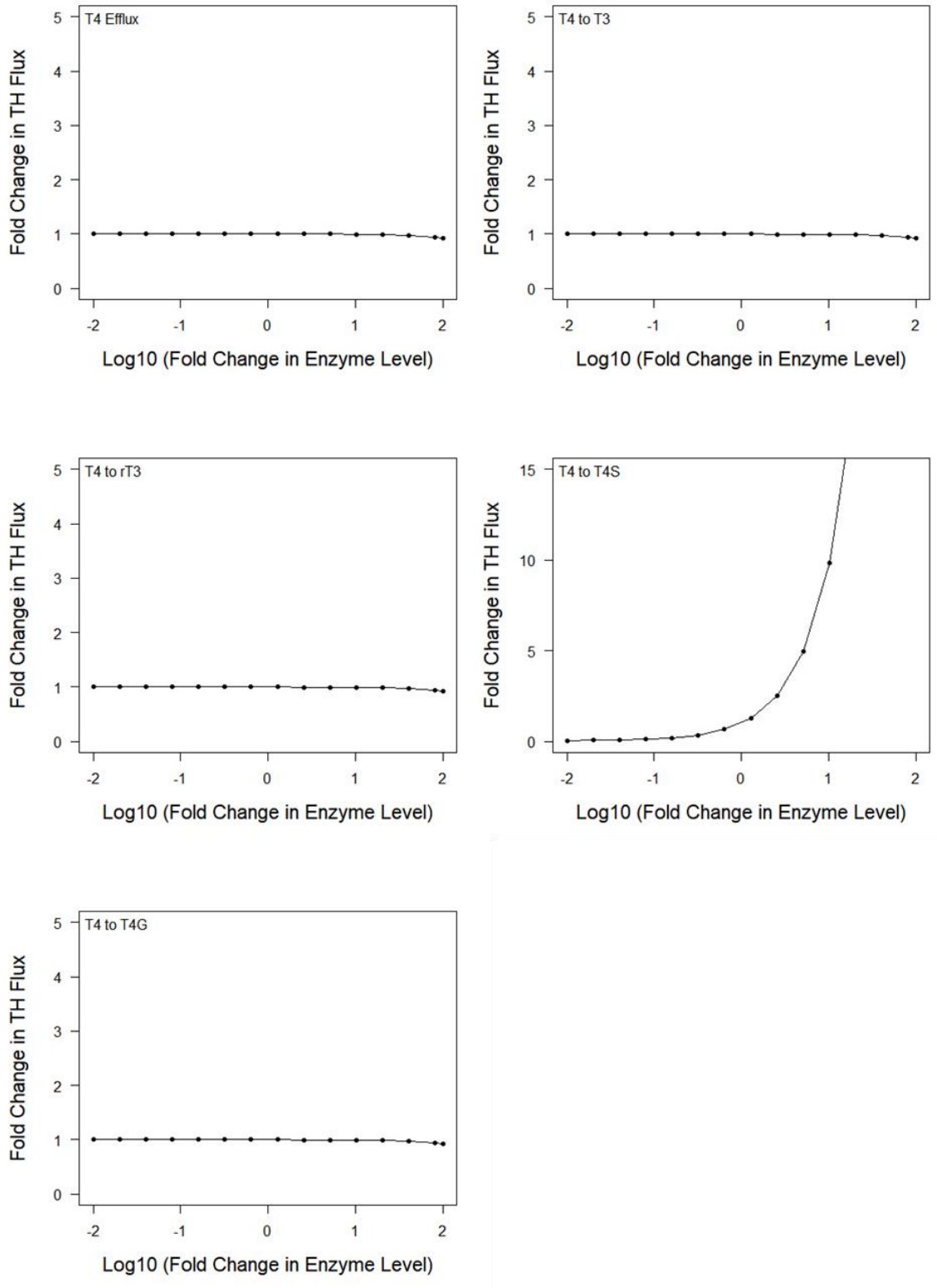

Figure 11. Steady-state dose-response of T_4 fluxes to changes in SULT1A1 in the liver.

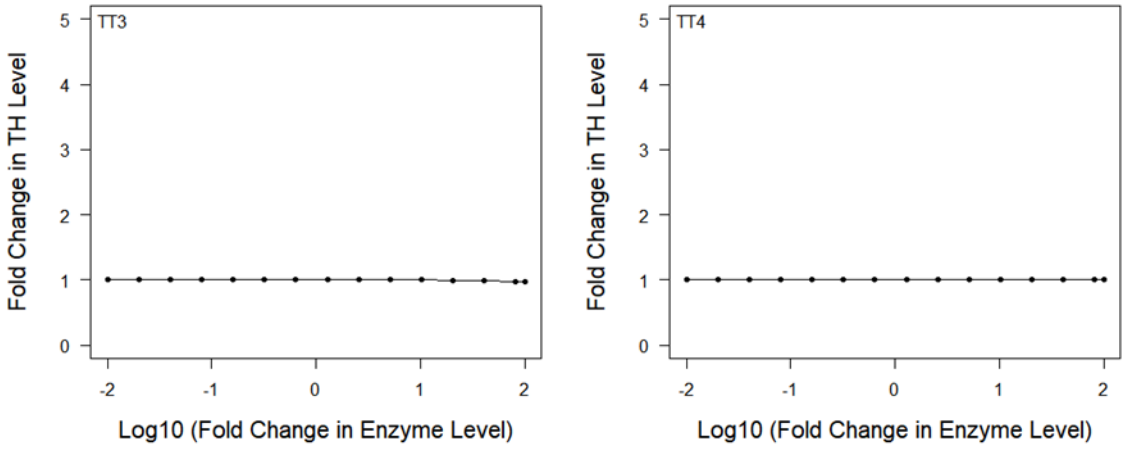

Figure 12. Steady-state dose-response of T_3 and T_4 to changes in SULT1E1 in the liver.

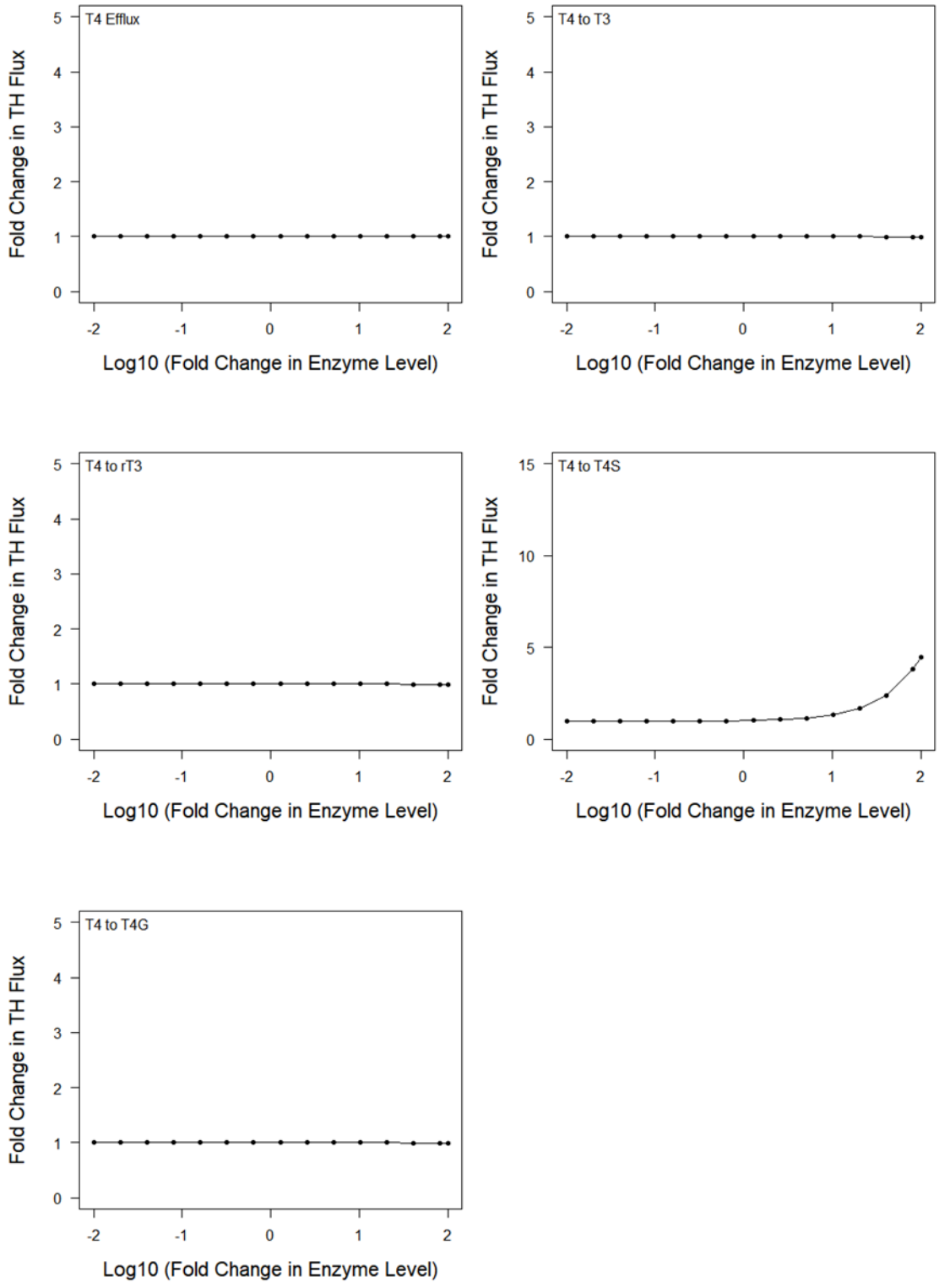

Figure 13. Steady-state dose-response of T_4 fluxes to changes in SULT1E1 in the liver.

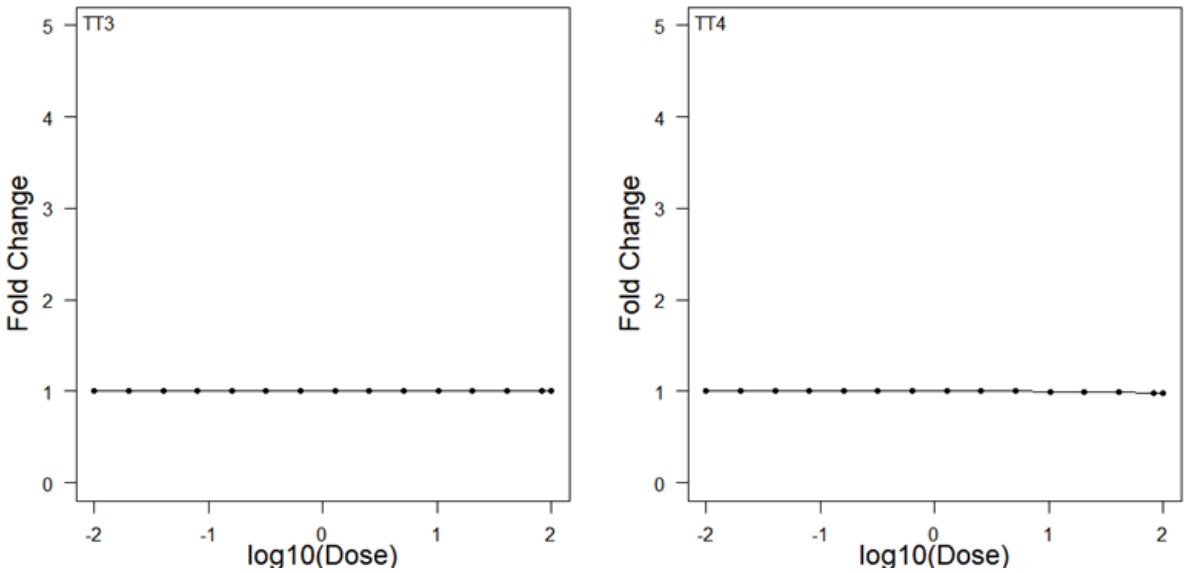

Figure 14. Steady-state dose-response of T_3 and T_4 to changes in UGT1A1 in the liver.

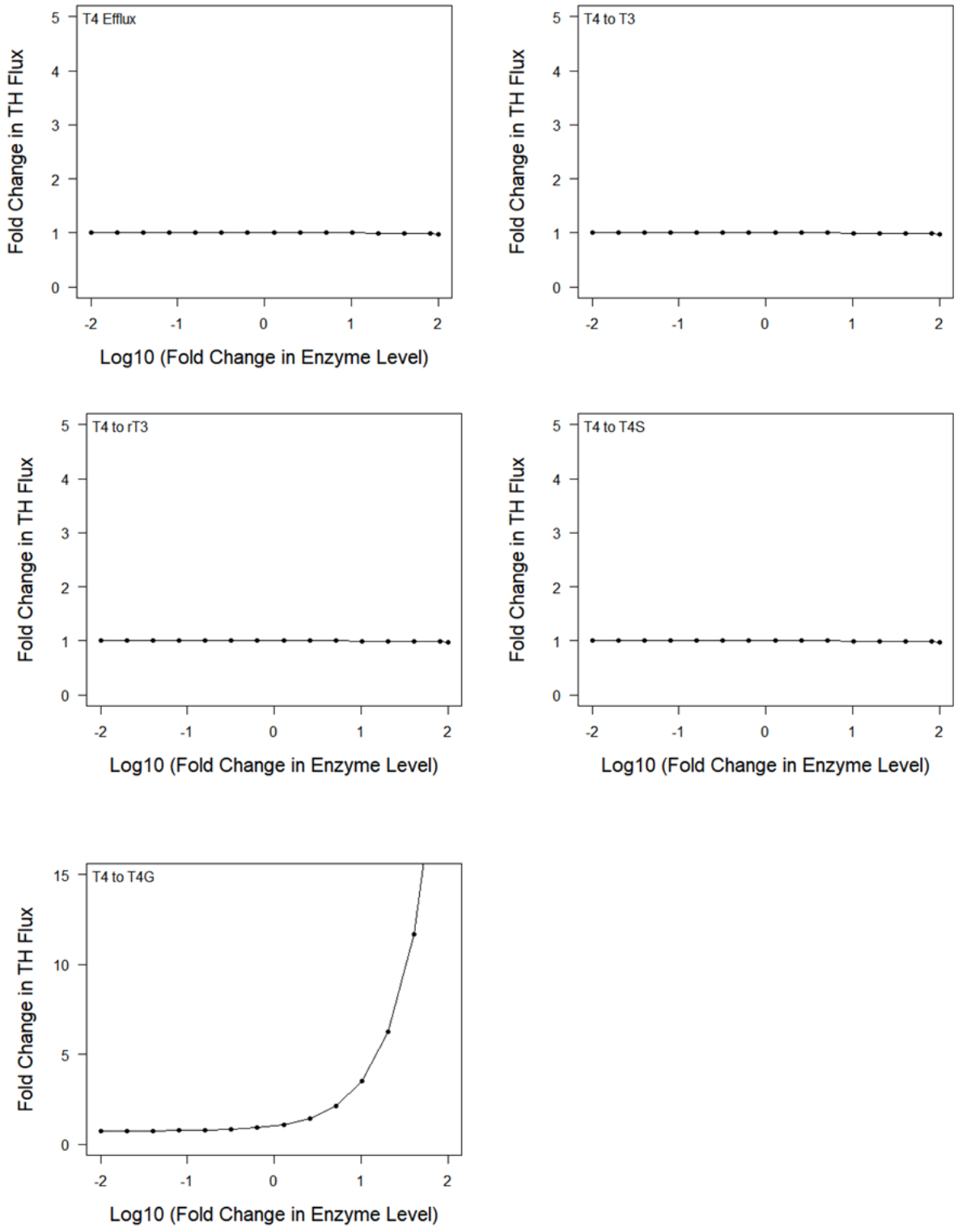

Figure 15. Steady-state dose-response of T_4 fluxes to changes in UGT1A1 in the liver.

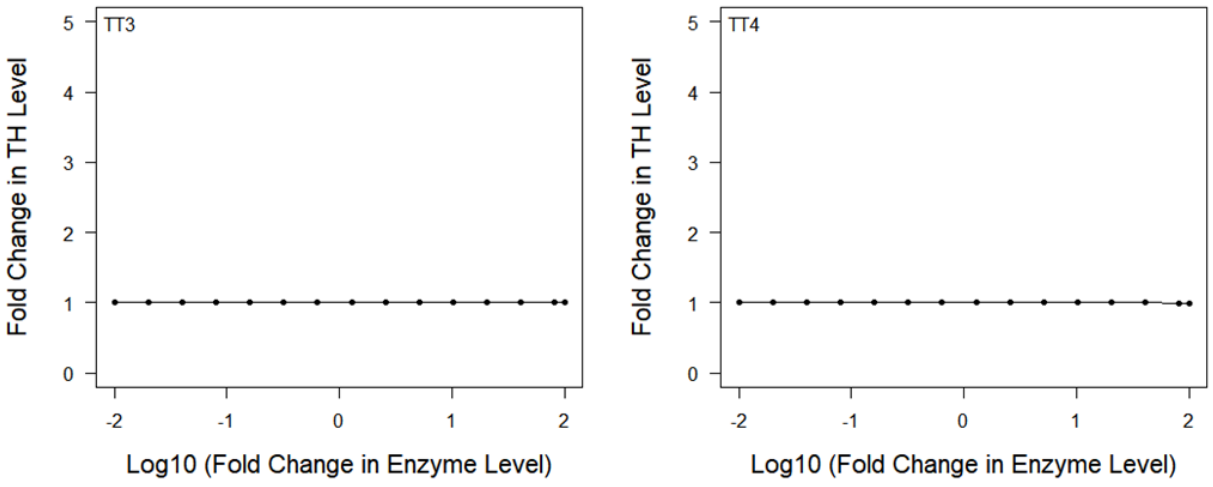

Figure 16. Steady-state dose-response of T_3 and T_4 to changes in UGT1A3 in the liver.

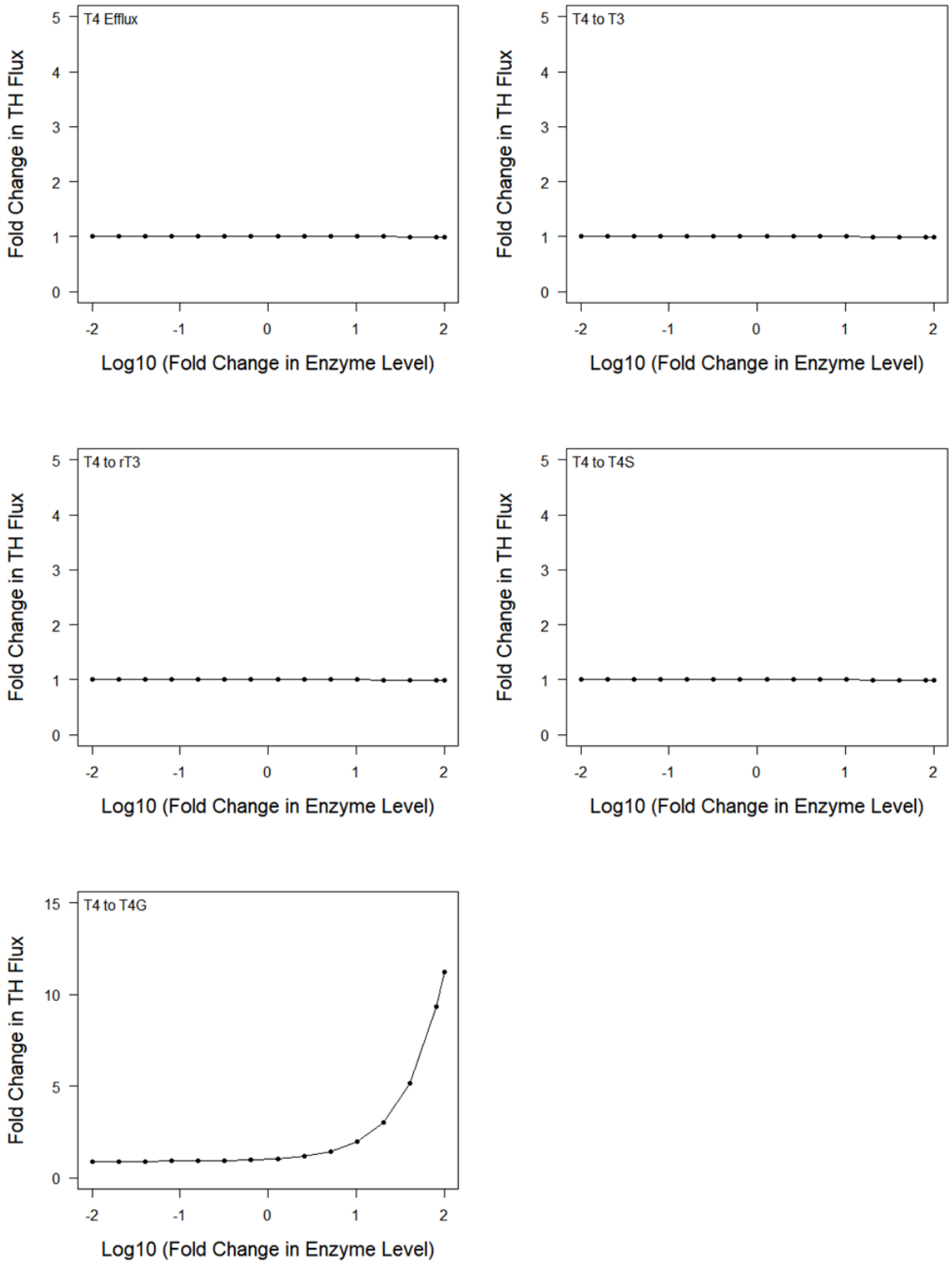

Figure 17. Steady-state dose-response of T_4 fluxes to changes in UGT1A3 in the liver.

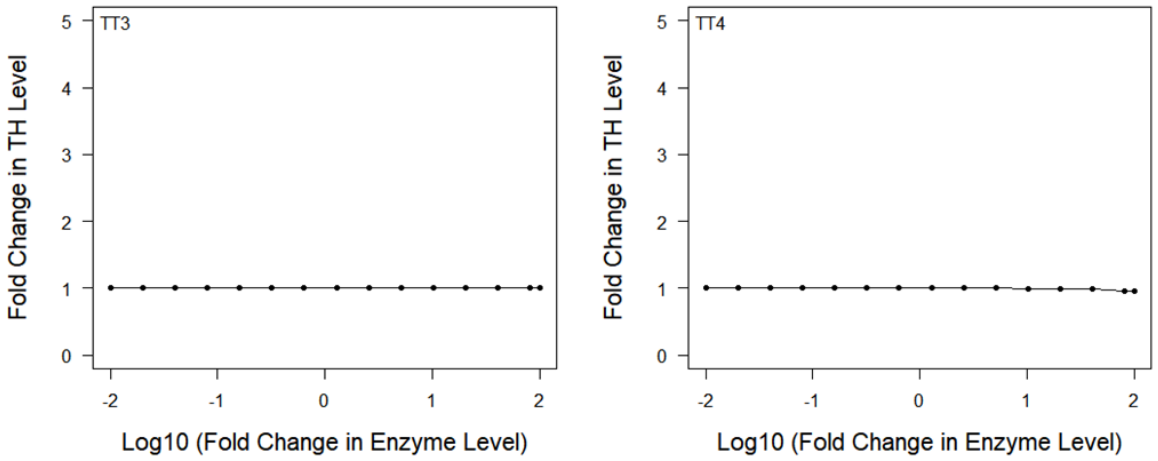

Figure 18. Steady-state dose-response of T_3 and T_4 to changes in UGT1A9 in the liver.

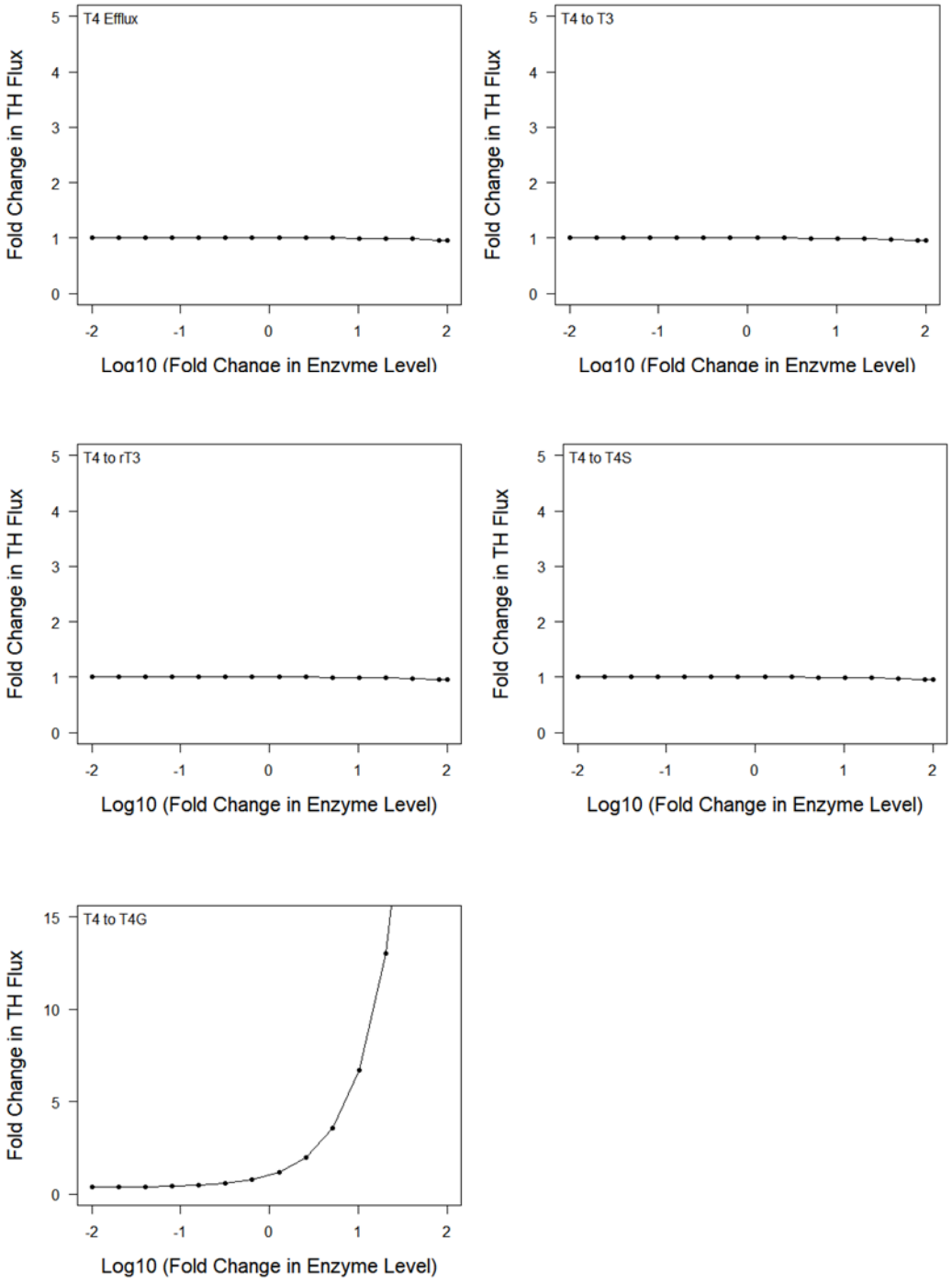

Figure 19. Steady-state dose-response of T_4 fluxes to changes in UGT1A9 in the liver.

Table1. Parameter Values (*Unadjusted)

Paramter Name	Value	Unit	Definition
VLT	1.7155	L	Total liver volumn for 75kg body weight adult
PT4	0.0004		Fraction of total T4 participates in the reactions in the liver
PT3	0.005		Fraction of total T3 participates in the reactions in the liver
Ft4_plasma	0.015	uM	Plasma's free T4 concentration
Ft3_plasma	0.005	uM	Plasma's free T3 concentration
KiT4	456	L/min	T4 influx rate from plasma into liver
KiT3	149.63	L/min	T3 influx rate constant from plasma into liver
KoT4	75.15	L/min	T4 efflux rate constant from liver into plasma
KoT3	42.48572	L/min	T3 efflux rate constant from liver into plasma
Deiodinase			
VmaxD1T4T3	236.52303	nmol/min/L liver	Maximum velocity of D1 and D2 in T4 to T3 conversion
KmD1T4T3	3350	uM	Michaelis constant of D1 and D2 in T4 to T3 conversion
VmaxD1T4rT3	208.263022	nmol/min/L liver	Maximum velocity of D1 in T4 to rT3 conversion
KmD1T4rT3	2950	uM	Michaelis constant of D1 in T4 to rT3 conversion
VmaxD1T3T2	19576	nmol/min/L liver	Maximum velocity of D1 in T3 to T2 conversion
KmD1T3T2	60	uM	Michaelis constant of D1 in T3 to T2 conversion
VmaxD1rT3T2	313	nmol/min/L liver	Maximum velocity of D1 in rT3 to T2 conversion*
KmD1rT3T2	2750	uM	Michaelis constant of D1 in rT3 to T2 conversion
VmaxD1T4SrT3S	18420	nmol/min/L liver	Maximum velocity of D1 in T4S to rT3S conversion*
KmD1T4rT3	300	uM	Michaelis constant of D1 in T4S to rT3S conversion
VmaxD1rT3ST2S	18070	nmol/min/L liver	Maximum velocity of D1 in rT3S to T2S conversion*
KmD1rT3ST2S	60	uM	Michaelis constant of D1 in rT3S to T2S conversion
VmaxD1T3ST2S	36770	nmol/min/L liver	Maximum velocity of D1 in T3S to T2S conversion*
KmD1T3ST2S	4600	uM	Michaelis constant of D1 in T3S to T2S conversion
Sulfotransferase			
VmaxSULT1A1T4	5689.44266	nmol/min/L liver	Maximum velocity of SULT1A1 in T4 sulfation
KmSULT1A1T4	167000	uM	Michaelis constant of SULT1A1 in T4 sulfation
VmaxSULT1E1T4	29.0986762	nmol/min/L liver	Maximum velocity of SULT1E1 in T4 sulfation
KmSULT1E1T4	23600	uM	Michaelis constant of SULT1E1 in T4 sulfation
VmaxSULT1A1T3	13500	nmol/min/L liver	Maximum velocity of SULT1A1 in T3 sulfation

KmSULT1A1T3	92850	uM	Michaelis constant of SULT1A1 in T3 sulfation
VmaxSULT1B1T3	17136	nmol/min/L liver	Maximum velocity of SULT1B1 in T3 sulfation
KmSULT1B1T3	142000	uM	Michaelis constant of SULT1B1 in T3 sulfation
VmaxSULT1E1T3	178.02	nmol/min/L liver	Maximum velocity of SULT1E1 in T3 sulfation
KmSULT1E1T3	25700	uM	Michaelis constant of SULT1E1 in T3 sulfation
VmaxSULT2A1T3	99.6	nmol/min/L liver	Maximum velocity of SULT2A1 in T3 sulfation
KmSULT2A1T3	14300	uM	Michaelis constant of SULT2A1 in T3 sulfation
VmaxSULT1E1rT3	3.125	nmol/min/L liver	Maximum velocity of SULT1E1 in rT3 sulfation*
KmSULT1E1rT3	2150	uM	Michaelis constant of SULT1E1 in rT3 sulfation
VmaxSULT2A1rT3	0.000333	nmol/min/L liver	Maximum velocity of SULT2A1 in rT3 sulfation*
KmSULT2A1rT3	7050	uM	Michaelis constant of SULT2A1 in rT3 sulfation
VmaxSULT1A1T2	0.2325	nmol/min/L liver	Maximum velocity of SULT1A1 in T2 sulfation*
KmSULT1A1T2	570	uM	Michaelis constant of SULT1A1 in T2 sulfation
VmaxSULT1B1T2	3.0145	nmol/min/L liver	Maximum velocity of SULT1B1 in T2 sulfation*
KmSULT1B1T2	7740	uM	Michaelis constant of SULT1B1 in T2 sulfation
VmaxSULT1E1T2	6.05	nmol/min/L liver	Maximum velocity of SULT1E1 in T2 sulfation*
KmSULT1E1T2	4750	uM	Michaelis constant of SULT1E1 in T2 sulfation
VmaxSULT2A1T2	0.002125	nmol/min/L liver	Maximum velocity of SULT2A1 in T2 sulfation*
KmSULT2A1T2	25675	uM	Michaelis constant of SULT2A1 in T2 sulfation
Glucotransferase			
VmaxUGT1A1T4	1003.520137	nmol/min/L liver	Maximum velocity of UGT1A1 in T4 glucordination
KmUGT1A1T4	104900	uM	Michaelis constant of UGT1A1 in T4 glucordination
VmaxUGT1A3T4	122.3805045	nmol/min/L liver	Maximum velocity of UGT1A3 in T4 glucordination
KmUGT1A3T4	33200	uM	Michaelis constant of UGT1A3 in T4 glucordination
VmaxUGT1A9T4	531.3796978	nmol/min/L liver	Maximum velocity of UGT1A9 in T4 glucordination
KmUGT1A9T4	24100	uM	Michaelis constant of UGT1A9 in T4 glucordination